

Marco Ceccarelli
Victor A. Glazunov *Editors*

Advances on Theory and Practice of Robots and Manipulators

Proceedings of ROMANSY 2014 XX
CISM-IFTToMM Symposium on Theory
and Practice of Robots and Manipulators

Mechanisms and Machine Science

Volume 22

Series editor

Marco Ceccarelli, Cassino, Italy

For further volumes:

<http://www.springer.com/series/8779>

Marco Ceccarelli · Victor A. Glazunov
Editors

Advances on Theory and Practice of Robots and Manipulators

Proceedings of ROMANSY 2014 XX
CISM-IFTToMM Symposium on Theory
and Practice of Robots and Manipulators

 Springer

Editors

Marco Ceccarelli
Laboratory of Robotics
and Mechatronics LARM
University of Cassino and South Latium
Cassino
Italy

Victor A. Glazunov
Mechanical Engineering Research
Institute, RAS
Moscow
Russia

ISSN 2211-0984

ISSN 2211-0992 (electronic)

ISBN 978-3-319-07057-5

ISBN 978-3-319-07058-2 (eBook)

DOI 10.1007/978-3-319-07058-2

Springer Cham Heidelberg New York Dordrecht London

Library of Congress Control Number: 2014939644

© Springer International Publishing Switzerland 2014

This work is subject to copyright. All rights are reserved by the Publisher, whether the whole or part of the material is concerned, specifically the rights of translation, reprinting, reuse of illustrations, recitation, broadcasting, reproduction on microfilms or in any other physical way, and transmission or information storage and retrieval, electronic adaptation, computer software, or by similar or dissimilar methodology now known or hereafter developed. Exempted from this legal reservation are brief excerpts in connection with reviews or scholarly analysis or material supplied specifically for the purpose of being entered and executed on a computer system, for exclusive use by the purchaser of the work. Duplication of this publication or parts thereof is permitted only under the provisions of the Copyright Law of the Publisher's location, in its current version, and permission for use must always be obtained from Springer. Permissions for use may be obtained through RightsLink at the Copyright Clearance Center. Violations are liable to prosecution under the respective Copyright Law. The use of general descriptive names, registered names, trademarks, service marks, etc. in this publication does not imply, even in the absence of a specific statement, that such names are exempt from the relevant protective laws and regulations and therefore free for general use.

While the advice and information in this book are believed to be true and accurate at the date of publication, neither the authors nor the editors nor the publisher can accept any legal responsibility for any errors or omissions that may be made. The publisher makes no warranty, express or implied, with respect to the material contained herein.

Printed on acid-free paper

Springer is part of Springer Science+Business Media (www.springer.com)

Preface

ROMANSY 2014, the 20th CISM-IFTToMM Symposium on Theory and Practice of Robots and Manipulators has been the twentieth event of a series that was started in 1973 as a first conference activity in the world on Robotics. The first event was held at International Centre for Mechanical Science (CISM) in Udine, Italy on 5–8 September 1973. It was also the first topic conference of International Federation for the Promotion of Mechanism and Machine Science (IFTToMM) and it was directed not only at the IFTToMM community.

The ROMANSY aim was decided at the funding meeting as a conference event representing a forum of reference for discussing the latest advances in Robotics and for facilitating contacts among research people, scholars, students, and professionals from the Industry. From the beginning the acronym ROMANSY was used to name the symposium in short by using the first letter of the words: Robots, Manipulators, and Symposium.

The aim of the ROMANSY Symposium is still focused to bring together researchers, industry professionals, and students from broad ranges of disciplines referring to Robotics, in an intimate, collegial, and stimulating environment. In 2014, after 41 years the ROMANSY event still is very attractive since we have received increased attention toward the initiative, as can be seen by the fact that this Proceedings volume contains contributions by authors from all around the world.

The funding committee that also took the responsibility for the organization of the first ROMANSY event was composed of:

- Prof. A. E. Kobrinskii (USSR); Chair
- Prof. L. Sobrero (Italy), Vice-Chair and CISM Director
- Acad. I. I. Artoboleveskii (USSR); first IFTToMM President
- Prof. G. Bianchi (Italy)
- Prof. I. Kato (Japan)
- Prof. M. S. Konstantinov (Bulgaria)
- Prof. A. Morecki (Poland)
- Prof. A. Romiti (Italy)
- Prof. B. Roth (USA)

Prof. M. W. Thring (UK)
 Dr. M. Vukobratovic (Jugoslavia)
 Prof. H. J. Warnecke (Germany)
 Prof. D. E. Withney (USA)
 Mrs. A. Bertozzi (Italy) acting as secretary as from CISM

The funders were the first generation in ROMANSY and they have been active for several decades. Smoothly, new generations have contributed to the leadership of ROMANSY by preserving the original characters of the initiative but challenging to increase the influence and spread of the ROMANSY results within a growing world Robotics community. The current scientific committee is listed below with names of persons who are from a third generation (since they started their activity after 2000) and others, who are even pupils of the funders.

The ROMANSY series was established as cooperation between IFToMM and CISM with an initial plan to have conference events alternatively at the CSIM headquarters in Udine, Italy, and in Poland under the direct responsibility of IFToMM and CISMM leaders together with the scientific committee. Later, as it is still today, it was decided to have the conference events hosted in any world institution where the organizing chair is active. The following is the list of ROMANSY events over time:

- 1973: ROMANSY 1 in Udine, Italy with chairmanship of A. E. Kobrinskii
- 1976: ROMANSY 2 in Jadwisin, Poland with chairmanship of B. Roth
- 1978: ROMANSY 3 in Udine, Italy with chairmanship of L. Sobrero
- 1981: ROMANSY 4 in Zaborow, Poland with chairmanship of A. Morecki
- 1984: ROMANSY 5 in Udine, Italy with chairmanship of G. Bianchi
- 1986: ROMANSY 6 in Cracow, Poland with chairmanship of A. Morecki
- 1988: ROMANSY 7 in Udine, Italy with chairmanship of G. Bianchi and A. Morecki
- 1990: ROMANSY 8 in Cracow, Poland with chairmanship of A. Morecki and G. Bianchi
- 1992: ROMANSY 9 in Udine, Italy with chairmanship of G. Bianchi and A. Morecki
- 1994: ROMANSY 10 in Gdansk, Poland with chairmanship of A. Morecki and G. Bianchi
- 1996: ROMANSY 11 in Udine, Italy with chairmanship of G. Bianchi and A. Morecki
- 1998: ROMANSY 12 in Paris, France with chairmanship of A. Morecki and G. Bianchi and J. C. Guinot
- 2000: ROMANSY 13 in Zakopane, Poland with chairmanship of A. Morecki and G. Bianchi
- 2002: ROMANSY 14 in Udine, Italy with chairmanship of G. Bianchi and J. C. Guinot

- 2004: ROMANSY 15 in Montreal, Canada with chairmanship of J. Angeles and J. C. Piedboeuf
- 2006: ROMANSY 16 in Warsaw, Poland with chairmanship of T. Zielinska
- 2008: ROMANSY 17 in Tokyo, Japan with chairmanship of A. Takanishi and Y. Nakamura
- 2010: ROMANSY 18 in Udine, Italy with chairmanship of W. Schiehlen and V. Parenti-Castelli
- 2012: ROMANSY 19 in Paris, France with chairmanship of P. Bidaud and O. Khatib

Proceedings volumes have been always published to be available also after the symposium to large public of scholars and designers.

This Proceedings volume contains 62 papers that have been selected after review for oral presentation and one invited lecture that prepared by Prof. Bernard Roth to celebrate the 20th anniversary event with his vision and memories. These papers cover several aspects of the wide field of Robotics concerning Theory and Practice of Robots and Manipulators.

We would like to express grateful thanks to the members of the current International Scientific Committee for ROMANSY Symposium for cooperating enthusiastically for the success of the 2014 event:

Philippe Bidaud (France)
 Marco Ceccarelli (Italy)
 I-Ming Chen (Singapore), as Chair of the IFToMM Technical Committee for Robotics and Mechatronics
 Victor Glazunov (Russia)
 Qian Huang (China)
 Oussama Khatib (USA)
 Vincenzo Parenti-Castelli (Italy), CISM representative
 Werner Schiehlen (Germany)
 Atsuo Takanishi (Japan)
 Teresa Zielińska (Poland)

We thank the authors who have contributed with very interesting papers on several subjects, covering many fields of Robotics as Theory and Practice of Robots and Manipulators and additionally for their cooperation in revising papers in a short time in agreement with reviewers' comments. We are grateful to the reviewers for the time and efforts they spent in evaluating the papers with a tight schedule that has permitted the publication of this proceedings volume in time for the symposium.

We thank the Blagonravov Institute of Machines Science (known also as IMASH) of Russian Academy of Science (RAS) in Moscow for having hosted the

ROMANSY 2014 event. We express our special thanks to academician Rivner Ganiev, director of IMASH, for supporting the hosting of ROMANSY 2014 in IMASH.

We would like to thank the members of the Organizing Committee: Academician, Prof. Vasilij Fomin; Mem. RAS., Prof. Alexandr Shplyuk; Mem. RAS., Prof. Vacheslav Prihodko; Mem. RAS., Prof. Nikolay Bolotnik; Prof. Veniamin Goldfarb; Prof. Irina Demianushko; Prof. Vigen Arakelian; Prof. Alexandr Golovin; Prof. Sergey Yatsun; Prof. Sergey Gavryushin; Prof. Sergey Misyurin; Dr. Raphael Sukhorukov; Prof. Saygid Uvaisov; Prof. Alexey Borisov; Prof. Anrey Korabelnikov; Dr. Oleg Muguin, Dr. Constantin Salamandra; Dr. Nikolay Tatus for their help in the plans for ROMANSY 2014 in Moscow.

We also thank the support of International Federation for the Promotion of Mechanism and Machine Science (IFTToMM) and the auspices of Centre for Mechanical Science (CISM). The long cooperation between IFTToMM and CISM has ensured and will ensure the continuous success of ROMANSY as a unique conference event in the broad area of Robotics with tracking reached achievements and future challenges. Special thanks are expressed to IFTToMM Russia that very enthusiastically supported the plan to have ROMANSY in Moscow and promoted a significant participation of Russian colleagues.

We thank the publisher and Editorial staff of Springer and particularly Dr. Nathalie Jacobs, managing Editor, for accepting and helping in the publication of this volume within the book series on Mechanism and Machine Science (MMS).

We are grateful to our families since without their patience and understanding it would not have been possible for us to organize ROMANSY-2014, the 20th CISM-IFTToMM Symposium on Theory and Practice of Robots and Manipulators.

Moscow, March 2014

Marco Ceccarelli
Victor A. Glazunov

Contents

Ro. Man. Sy.: Its Beginnings and Its Founders	1
B. Roth	
Parametric Method for Motion Analysis of Manipulators with Uncertainty in Kinematic Parameters	9
Vahid Nazari and Leila Notash	
Self-Adjusting Isostatic Exoskeleton for the Elbow Joint: Mechanical Design	19
V. A. Dung Cai and Philippe Bidaud	
Design of Ankle Rehabilitation Mechanism Using a Quantitative Measure of Load Reduction	27
Daisuke Matsuura, Shouta Ishida, Tatsuya Koga and Yukio Takeda	
Characterization of the Subsystems in the Special Three-Systems of Screws	37
Dimiter Zlatanov and Marco Carricato	
Singularity Analysis of 3-DOF Translational Parallel Manipulator	47
Pavel Laryushkin, Victor Glazunov and Sergey Demidov	
Generalised Complex Numbers in Mechanics	55
J. Rooney	
On the Perturbation of Jacobian Matrix of Manipulators	63
Leila Notash	
Accuracy Improvement of Robot-Based Milling Using an Enhanced Manipulator Model	73
Alexandr Klimchik, Yier Wu, Stéphane Caro, Benoît Furet and Anatol Pashkevich	

Design and Optimization of a Tripod-Based Hybrid Manipulator	83
Dan Zhang and Bin Wei	
Moving Mechanism Design and Analysis of Suspension Insulator Inspection Robot.	93
Shujun Li, Hongguang Wang, Shichao Xiu, Xiaopeng Li and Zhaohui Ren	
Design of 4-DOF Parallelogram-Based RCM Mechanisms with a Translational DOF Implemented Distal from the End-Effector	103
A. Gijbels, D. Reynaerts and E. B. Vander Poorten	
Rotational Axes Analysis of the 2-RPU/SPR 2R1T Parallel Mechanism	113
Yundou Xu, Shasha Zhou, Jiantao Yao and Yongsheng Zhao	
Recursive and Symbolic Calculation of the Stiffness and Mass Matrices of Parallel Robots	123
Sébastien Briot and Wisama Khalil	
Kinematics, Dynamics, Control and Accuracy of Spherical Parallel Robot.	133
Sergey Kheylo and Victor Glazunov	
Dynamics and Control of a Two-Module Mobile Robot on a Rough Surface.	141
N. Bolotnik, M. Pivovarov, I. Zeidis and K. Zimmermann	
Shaking Force and Shaking Moment Balancing in Robotics: A Critical Review	149
Vigen Arakelian	
Investigation into the Influence of the Foot Attachment Point in the Body on the Four-Link Robot Jump Characteristics.	159
S. Jatsun, O. Loktionova, L. Volkova and A. Yatsun	
Numerical Detection of Inactive Joints.	167
Marek Wojtyra	
Quasi-Static Motions of a Three-Body Mechanism Along a Plane	175
I. Borisenko, F. Chernousko and T. Figurina	

Control Design for 3D Flexible Link Mechanisms Using Linearized Models 181
 Erfan Shojaei Barjuei, Paolo Boscariol, Alessandro Gasparetto, Marco Giovagnoni and Renato Vidoni

Walking on Slippery Surfaces: Generalized Task-Prioritization Framework Approach 189
 Milutin Nikolić, Borovac Branislav and Mirko Raković

Autonomous Robot Control in Partially Undetermined World via Fuzzy Logic. 197
 S. Yu. Volodin, B. B. Mikhaylov and A. S. Yuschenko

Laplacian Trajectory Vector Fields for Robotic Movement Imitation and Adaption 205
 Thomas Nierhoff, Sandra Hirche and Yoshihiko Nakamura

Trajectory Planning of Redundant Planar Mechanisms for Reducing Task Completion Duration 215
 Emre Uzunoğlu, Mehmet İsmet Can Dede, Gökhan Kiper, Ercan Mastar and Tayfun Sığirtmaç

Design Choices in the Development of a Robotic Head: Human-Likeness, Form and Colours 225
 Scean Mitchell, Gabriele Trovato, Matthieu Destephe, Massimiliano Zecca, Kenji Hashimoto and Atsuo Takanishi

Hopping Robot Using Pelvic Movement and Leg Elasticity 235
 Takuya Otani, Kazuhiro Uryu, Masaaki Yahara, Akihiro Iizuka, Shinya Hamamoto, Shunsuke Miyamae, Kenji Hashimoto, Matthieu Destephe, Masanori Sakaguchi, Yasuo Kawakami, Hun-ok Lim and Atsuo Takanishi

A Robotic Head that Displays Japanese “Manga” Marks 245
 Tatsuhiro Kishi, Hajime Futaki, Gabriele Trovato, Nobutsuna Endo, Matthieu Destephe, Sarah Cosentino, Kenji Hashimoto and Atsuo Takanishi

Terrain-Adaptive Biped Walking Control Using Three-Point Contact Foot Mechanism Detectable Ground Surface 255
 Kenji Hashimoto, Hyun-jing Kang, Hiromitsu Motohashi, Hun-ok Lim and Atsuo Takanishi

Biped Walking on Irregular Terrain Using Motion Primitives	265
Mirko Raković, Branislav Borovac, Milutin Nikolić and Srđan Savić	
Experimental Investigation of Human Exoskeleton Model.	275
V. G. Gradetsky, I. L. Ermolov, M. M. Knyazkov, E. A. Semyonov and A. N. Sukhanov	
Underactuated Finger Mechanism for LARM Hand.	283
M. Zottola and M. Ceccarelli	
Design and Kinematic Analysis of a Novel Cable-Driven Parallel Robot for Ankle Rehabilitation	293
Runtian Yu, Yuefa Fang and Sheng Guo	
Position/Force Control of Medical Robot Interacting with Dynamic Biological Soft Tissue.	303
V. Golovin, M. Arkhipov and V. Zhuravlev	
Biomimicking a Brain-Map Based BCF Mode Carangiform Swimming Behaviour in a Robotic-Fish Underwater Vehicle.	311
Abhra Roy Chowdhury and S. K. Panda	
Variable Inertia Muscle Models for Musculoskeletal Dynamics.	321
Minyeon Han and F. C. Park	
UGV Epi.q-Mod	331
Giuseppe Quaglia, Luca G. Butera, Emanuele Chiapello and Luca Bruzzone	
Six-Link In-pipe Crawling Robot.	341
S. Jatsun, O. Loktionova and A. Malchikov	
Dynamics Model of STB Projectile Loom.	349
Assylbek Jomartov, Skanderbek Joldasbekov and Gakhip Ualiyev	
Development of an Origami Type Robot to Realize Transformation and Movement	357
Kazuma Otani and Mitsuharu Matsumoto	
From Lawnmower Dynamics to Modeling, Simulation and Experiments of a Differentially Driven Robot.	365
Qirong Tang and Werner Schiehlen	

Kinematic Analysis Validation and Calibration of a Haptic Interface 375
 Mehmet İsmet Can Dede, Barış Taner, Tunç Bilginçan and Marco Ceccarelli

Problems of Increasing Efficiency and Experience of Walking Machines Elaborating 383
 E. S. Briskin, V. A. Shurygin, V. V. Chernyshev, A. V. Maloletov, N. G. Sharonov, Y. V. Kalinin, A. V. Leonard, V. A. Serov, K. B. Mironenko and S. A. Ustinov

Stiffness Analysis of WL-16RV Biped Walking Vehicle 391
 Giuseppe Carbone, Kenji Hashimoto and Atsuo Takanishi

Compliance Based Characterization of Spherical Flexure Hinges for Spatial Compliant Mechanisms 401
 Farid Parvari Rad, Giovanni Berselli, Rocco Vertechy and Vincenzo Parenti Castelli

Analysis and Synthesis of Thin-Walled Robot Elements with the Guided Deformation Law 411
 S. Gavryushin

HCLC Integration Design and High-Precision Control of a Joint for Space Manipulator 419
 Zhihong Jiang, Hui Li, Que Dong, Xiaodong Zhang, Zixing Tang, Wei Rao, Yang Mo, Chenjun Ji and Qiang Huang

A Novel Robotic Joint Actuation Concept: The Variable Mechanical Fuse, VMF 427
 Yoichiro Dan and Oussama Khatib

Internal Force-Based Impedance Control for Cable-Driven Parallel Robots 435
 C. Reichert, K. Müller and T. Bruckmann

Time Sub-Optimal Path Planning for Hyper Redundant Manipulators Amidst Narrow Passages in 3D Workspaces 445
 Elias K. Xidias and Nikos A. Aspragathos

A Blocking Plate Manipulation Robot System Based on Image Recognition 453
 Yonggui Wang, Xingguang Duan, Amjad Ali Syed, Meng Li, Xiangzhan Kong, Chang Li, Yang Yang and Ningning Chen

Walking Mobile Robot with Manipulator-Tripod	463
V. Zhoga, A. Gavrilov, V. Gerasun, I. Nesmianov, V. Pavlovsky, V. Skakunov, V. Bogatyrev, D. Golubev, V. Dyashkin-Titov and N. Vorobieva	
Brain Flow in Application for New Robotic POLIMI Platform	473
Alberto Rovetta	
A Dual Formation Constraint Mechanism of Mobile Sensor Network Based on Congestion Will	483
Cheng Yang, Ping Song, Chuangbo Hao, Guang Wang, Lin Xie and Wenjuan Guo	
Kinematic Uncertainties in Human Motion Tracking and Interaction	491
Qilong Yuan and I-Ming Chen	
Experiments of a Human-Robot Social Interactive System with Whole-Body Movements	501
Gan Ma, Qiang Huang, Zhangguo Yu, Xuechao Chen, Weimin Zhang, Junyao Gao, Xingguang Duan and Qing Shi	
Distributing the Supporting Heads for Robotized Machining	509
Teresa Zielinska, Wlodzimierz Kasprzak, Cezary Zielinski and Wojciech Szykiewicz	
The Founder of Russian School of a Robotics (to the 100 Anniversary Since the Birth of Academician E. P. Popov)	519
Evgeny Kotov, Anaid Nazarova and Sergey Vorotnikov	
Scaffold with Improved Construction Rigidity	527
Y. S. Temirbekov and S. U. Joldasbekov	
Force Capability Polytope of a 3RRR Planar Parallel Manipulator	537
L. Mejia, H. Simas and D. Martins	
Interactive Design of a Controlled Driving Actuator	547
G. V. Kreinin and S. Yu. Misyurin	

Design and Implementation of Self-Balancing Camera Platform for a Mobile Robot 555
Mehmet Volkan Bukey, Emin Faruk Kececi and Aydemir Arısoy

Action of Robot with Adaptive Electric Drives of Modules 563
Konstantin S. Ivanov

Author Index 571

Ro. Man. Sy.: Its Beginnings and Its Founders

B. Roth

Abstract This paper describes the origins of the ROMANSY series of symposia. It recounts the author's experience as one of the original founders. The emphasis is on the events leading to the first organizational meetings and the people involved in organizing the early symposia.

Keywords ROMANSY · CISM · IFToMM · Robot · Symposia

1 Introduction

My purpose in writing this paper is to record my personal recollections of the events that led to the founding of the Romansy symposia. I undertook this task at the kind invitation of Professors V. Glazunov and M. Ceccarelli. As organizers of the 20th symposium in the Romansy series, they felt it would be appropriate to mark this anniversary by adding an historical perspective. The task fell to me since, sadly, I am the last living member of the original group that conceived the project and issued the invitations to form the first Organizing Committee.

I do want to point out that Moscow is an especially appropriate venue for this 20th anniversary event since three prominent academics from Moscow, Academician I. I. Artobolevskii, Professor A. P. Bessonov and Professor A. E. Kobrinskii, played pivotal roles in Romansy's establishment and early implementations.

B. Roth (✉)
Stanford University, Standford, CA, USA
e-mail: broth@stanford.edu

2 My Voyage

Every event has many antecedents. Depending on the narrator, different founding stories start at different points in time. This paper is my version of what happened. I am fully aware that the other founders would have their own versions. Their stories would certainly overlap mine, yet this version could only be seen through my perspective. For me the essential part of the founding of Romansy began when my wife and I visited the Soviet Union for 30 days, starting April 7, 1969, under a USA-USSR Academy of Science exchange program. We were met at the airport by Professor Arcady Bessonov.

During that visit I met Professor Aaron Kobrinskii for the first time, and learned about his work in computer-aided manufacturing, vibrations, mechanisms and robotics. Most importantly, I met Academician Ivan Ivanovich Artobolevskii. I did not fully realize what an important figure Artobolevskii was until I was invited to lunch at his apartment and saw that he lived in a very prestigious location close to the Kremlin. I later found out that in addition to his academic achievements he had been elected to one of the top government bodies: the Supreme Soviet.

The next important connection for the role I was to play in the founding of Romansy occurred when we stopped for a two-week visit in Bulgaria on our way back from the USSR. Our host there was Professor Michael Konstantinov. He had been educated in a German school in Sofia, and his German was much better than his English. So, German was the language we mainly used. As an aside, his German was so beautifully and clearly spoken, that being with him was for me like attending an intensive and highly productive German refresher course.

The final steps in my personal voyage toward the formation of Romansy occurred four months later at the Second IFToMM International Congress on the Theory of Machines and Mechanisms that was held in Zakopane, Poland in September of 1969. I gave a paper on the kinematics of computer controlled manipulators that described some of the work I had been doing with my PhD student Donald Pieper. The presentation included a short film showing a computer controlled manipulator constructing a small tower of blocks while moving through an environment with obstacles that had to be avoided. It was the first autonomous manipulation demonstration that most people in the audience had ever seen. Such films are now commonplace. At that time however, it seemed excitingly new and forward looking.

At the IFToMM Congress Artobolevskii was somewhat of an aloof and imperial figure. He was housed separately and more luxuriously than the other participants. Generally he did not mix with participants during the off hours between sessions. However, when he attended technical sessions he always sat erectly in the front row and listened intently to the presentation.

When I gave my talk and showed my film he was in his usual front row seat. After my talk he came up to me, greeted me warmly and expressed, what seemed to me, very genuine admiration for my work. I could sense there was a strong interest on his part in further study on the topic of autonomous manipulation.

There were two other seemingly casual connections at this IFToMM Congress that later proved pivotal for the development of Romansy. They involved Professors Giovanni Bianchi and Adam Morecki. I had never met either of them before the Congress. Morecki was a professor at the Technical University in Warsaw who worked mainly in biomechanics and its application to medical rehabilitation. Bianchi's main interest was classical mechanics and its application to machine design. He was a professor at the Polytechnic in Milan.

The Romansy symposia were originated under the joint sponsorship of CISM and IFToMM. The founding of CISM and IFToMM both came to fruition after years of earlier discussion and organizational work. Both of these organizations were officially born at about the same time in the late 1960s. To understand the founding of Romansy it is useful to briefly review the connection of Romansy's founders to CISM and IFToMM.

3 CISM and IFToMM

CISM: The acronym is for the Italian rendering of International Center for Mechanical Sciences. Professor Luigi Sobrero was the longtime director of the Institute of Mechanics at the University of Trieste. In 1968, toward the end of a distinguished career, he succeeded in gathering enough support of eminent colleagues in Europe to establish CISM as an international institute for promoting post graduate study in the field of mechanics.

In order to foster economic growth in the region, the city of Udine gave CISM use of a palace that had been donated to it by Count Alessandro del Torso. His expressed wish was that it should be devoted to cultural activities. To this day, this palace, located in the heart of the city, provides office and meeting space for most of CISM's activities. Once established, CISM was governed by a board that consisted of representatives of member nations. One of these board members was appointed rector of CISM. It happened to be Professor Waclaw Olszak who had strong ties to his native Poland and the Polish scientific community. Especially important for Romansy was his close relationship with Adam Morecki. The other direct connection between CISM and Romansy was that Giovanni Bianchi was also deeply involved in CISM's governance and had close ties to its founder Luigi Sobrero.

IFToMM: Although it has now been modified, this acronym originally stood for the International Federation for the Theory of Mechanisms and Machines. Among the most active founders of IFToMM were Artobolevskii, Bessonov, and Konstantinov. In fact Artobolevskii was the founding president of IFToMM; Bessonov held various executive positions and Konstantinov was to become IFToMM's secretary general.

The financial arrangements were a bit unusual. IFToMM was funded by dues from member countries. It had a relatively small budget and could only make token contributions to Romansy. CISM received a land subsidy from the city of

Udine, but in the main it was also funded by dues from member countries. Some of the Eastern European countries paid their CISM dues in local non-dollar convertible currency. In particular CISM had resources it could make available for meetings that were held in Poland. That combined with Adam Morecki's organizational abilities created the early pattern of alternating the venue for Romansy between Udine and Poland. It also biased the venue of many of the organizing committee meetings to Poland.

4 Founders

I have outlined the circumstances that brought me into contact with the main originators of what became the Romansy symposia. The idea to organize an international symposium on robot research was brought to me by Kobrinskii in September 1971 during the Third IFToMM World Congress held in Kupari, Yugoslavia. Kobrinskii invited me to a meeting with Professor Sobrero, the founding Secretary General of CISM, and his secretary Mrs. A. Bertozzi. In addition to the four of us there were three other participants: Artobolevskii, Konstantinov and Bianchi. The seven of us held a meeting that what would in retrospect be the founding moment of Romansy. At this meeting we agreed to organize an international symposium. It was also decided that Kobrinskii would be the chairman of the organizing committee, and Sobrero would be the vice-chairman.

Artobolevskii assured us of IFToMM's support. Sobrero was anxious to grow activities at CISM and he wanted the symposium to take place at their headquarters in Udine.

We then had to decide what to call the proposed symposium. Kobrinskii who had a quick mind and enjoyed mental puzzles suggested Robot and Manipulator Symposium with the acronym ROMANSY. Bianchi objected. He felt the acronym was too frivolous and conveyed the wrong message. At the time, I did not know Bianchi well. I remember thinking, "there goes my stereotype of Italian lovers." We discussed this for a long time. Finally Bianchi acquiesced when we agreed to write the acronym as Ro. man. sy. Later, I became very close friends with Bianchi and his family. I realized that he had been brought up in a banking family with conservative social manners. This background caused Bianchi to have a visceral rejection of Kobrinskii's brilliant idea. Slowly over the years the acronym morphed into the original suggestion. First the spaces after the periods disappeared, and we had Ro.man.sy and also RO.MAN.SY. Next the periods disappeared and we got to RoManSy. Eventually the cover of the proceeding boldly proclaimed Kobrinskii's original ROMANSY.

The original meeting in Kupari was followed by a more extensive meeting in Nieborow, Poland in May 1972. The host for this meeting was Prof. Adam Morecki. He arranged for us to meet and live in the old Radzivil Palace, which now belonged to the Polish government. This venue fostered a very relaxed country atmosphere which provided opportunities for long strolls and off-the-record conversations.

In addition to Artobolevskii, Kobrinskii, Konstantinov, the meeting was attended by Prof. Medford Thring from University College, London, Adam Morecki from the Polytechnic of Warsaw, Miomir Vukobratović from Mihajlo Pupin Institute in Belgrade, Ikiro Khato from Wasada University, Tokyo. Giovanni Bianchi represented IFToMM and Luigi Sobrero and Mrs. Anna Bertozzi represented CISM. At this meeting we prepared the call for papers for the first symposium, which was set for September 1973 at CISM in Udine.

Figure 1 Shows a photo I took at that meeting. In the front row from left to right we have Kato, Artobolevskii, Sobrero, Konstantinov, and Thring. The second row has Bianchi and Bertozzi. The third row shows Morecki flanked by two staff members. The last row has two of Morecki's staff and Vukobratović on the right.

There was a final organizing meeting that took place in Split, Yugoslavia in April of 1973. This meeting was hosted by Professors Bazjanac and Jelovac from Zagreb. This meeting was attended by the same group as at Nieborow and, in addition, Professor Hans Wanecke from the University of Stuttgart and Professor Romiti from the Polytechnic in Turin.

At the Split meeting the submitted papers were reviewed. It was decided to accept 45 papers and publish them in a volume of conference preprints. I wanted the final proceedings to be as readable as possible. So, I went through all the papers written by non English speaking authors and, where necessary, annotated them with suggested language modifications. I still recall the gratitude I received when I passed out the edited manuscripts to the authors at the symposium.

5 First Symposium

The symposium was held on September 5–8, 1973 in the beautifully frescoed main hall of the Palazzo del Torso. All the papers were presented on a single track, so everyone was in the same sessions through the symposium.

After receiving the revisions, Mrs. Bertozzi arranged to have the final proceeding published as two-volume set by Springer-Verlag. The final proceedings contain the text of two Opening Lectures. The first one runs for a little over 7 pages. It is titled "The State of the Art in the field of Robots and Manipulators." It is signed A. E. Kobrinskii, Academy of Sciences of the USSR. The second one runs for two pages and is titled "Robots and Manipulators" it is signed by M. W. Thring, University of London. Whenever I look at this part of the proceedings I am reminded of what I consider the saddest event in the history of Romansy.

If there was a single person to be credited with the idea for Romansy it would be Kobrinskii. In recognition of this he was the chairman of the Organizing Committee for the first symposium. He attended all of the organizing committee meetings and was given the honor of presenting the opening lecture. It was unimaginable that he would not attend the symposium. Yet, when the scientists from the Soviet Union arrived, he was not among them. I was told that he had to cancel his trip at the last minute because his brother was stricken with an illness. It



Fig. 1 Organizing and program committee and staff, Nieborow, Poland in May 1972

was true that his trip had been cancelled at the last minute. However it had nothing to do with family illness. It was because he was not given an exit visa. I do not pretend to know the reason for this. I do know that Kobrinskii felt it was due to his Jewish origins and the Soviet Government's discriminative policies towards its Jewish citizens at that time.

These are not pleasant things to recall, especially in a paper meant to celebrate the cooperation between researchers from throughout the world. Kobrinskii is dead and so are most of the colleagues who attempted to hide the truth. In a cosmic sense the incident is meaningless. I mention it here mainly to emphasize the importance of Aaron Kobrinskii's role in Romansy's birth and to pay homage to an unusually creative colleague by acknowledging my empathy for what must have been an incredibly painful personal episode.

The rest of the symposium was uneventful and was full of good feelings and comradeship. We had achieved our goal of opening a multinational scientific exchange in the area of robotics. In addition to the two invited opening lectures, we had accepted 45 papers. The distribution according to country of these 45 papers was: USA 13, USSR 13, Japan 4, England 3, Yugoslavia 3, West Germany 3, Italy 2, Poland 2, Bulgaria 1, and France 1.

On the last day of the symposium the organizing committee was invited by Professor Sobrero to a lunch meeting in the restaurant of the upscale Astoria Hotel around the corner from CISM. I recall we were seated at a long rectangular table. Artobolevskii sat at the head and I was far away toward other end. We agreed that the symposium had been a success and that a second Romansy should be held in

Poland in 1976. The organizing committee was to have two meetings before the symposium, the first of which was to be in Warsaw in June of 1974.

The lunch went on a bit long and toward the end my mind was wandering. I was barely paying attention when Artobolevskii rose with wine glass in his hand and said, "I propose that Professor Roth should be the new chairman of the organizing committee". This was greeted with a round of applause. That was it, it was an imperial order and everyone obeyed. I was flabbergasted at Artobolevskii's action on two counts: I was both an American and the youngest person at the table. I suppose Artobolevskii must have discussed it with Sobrero and Bianchi beforehand, yet it always remained in my mind a personally generous gesture of great magnanimity on his part. I took it as both strengthening our personal connection and as a signal that Romansy had achieved a measure of Soviet-American cooperation that at the time was very much lacking in the world.

6 An Ongoing Series

The success of the first symposium led CISM and IFToMM to jointly form a permanent Technical Committee on Robots and Manipulators. This technical committee was to organize the second and all subsequent Romansy symposia. I had the honor to be the chair of this technical committee for its first years. For the second symposium the committee was:

Chairman: Prof. B. Roth (Stanford University), *Vice-Chairmen:* Prof. L. Sobrero (CISM), Prof. A. Morecki (Technical University of Warsaw). *Members:* Acad. I. I. Artobolevskii (Institute for the Study of Machines, Moscow), Prof. G. Bianchi (Technical University of Milan), Prof. I. Kato (Wasada University), Prof. A. E. Kobrinskii (Institute for the Study of Machines, Moscow), Prof. M. S. Konstantinov (High Mechanical and Electromechanical Institute, Sofia), Prof. R. B. McGhee (The Ohio State University), Prof. M. W. Thring (University of London), Mr. J. Vertut (Atomic Energy Commission, France), Prof. M. Vukobratović (Mihajlo Pupin Institute), Prof. H. J. Warnecke (University of Stuttgart). *Scientific Secretary:* Dr. K. Kędzior (Technical University of Warsaw). *Secretary:* Mrs. A. Bertozzi (CISM).

The Technical Davison of the Polish Academy of Sciences joined CISM and IFToMM's financial sponsorship, and two preparatory committee meetings for the second Romansy were held in Poland. The Second International CISM-IFToMM Symposium took place in the small village of Jadwisin near Warsaw, Poland on September 14–17, 1976. There was a volume of preprints available at the symposium.

The second Romansy was attended by 117 participants and 15 accompanying guests. They came from 4 continents and 20 countries (which doubled the 10 countries for the first symposium). The social programs included a banquet with groups of participants singing in various languages and a half-day excursion. This became the model for subsequent Romansy symposia.

For the second symposium we adopted the policy that a paper could only be published in the proceedings if it was actually presented at the symposium. I have always felt regret that this policy led to the exclusion of some good papers.

Artobolevskii passed away at the age of 71 on September 21, 1977, a year before the third Romansy. I happen to have been in the USSR at the time. I was attending a conference in Alma Ata. As soon as his death was announced everything seemed to shut down. Many participants hurried back to Moscow to attend his funeral. To me the most impressive reminder of what an important figure he was happened when the TV throughout the Soviet Union stopped its normal programs and simply played dirge music in his memory.

His colleague Prof. A. P. Bessonov had been acting as an aid-de-camp to Artobolevskii since the founding of Romansy. So, he was very knowledgeable about Romansy and was able to seamlessly take up Artobolevskii's role as a representative of the USSR on the Organizing Committee.

The third Romansy was held in Udine at CISM on September 12–15, 1978. About 8 months after the third symposium our great benefactor Prof. Luigi Sobrero passed away at the age of 69. CISM had been the crowning passion of his life, and he left it in very good shape as far as Romansy was concerned. Prof. Giovanni Bianchi had served as an aid-de-camp to Sobrero from the beginning of the Romansy discussions. After Sobrero died, he was appointed Secretary General of CISM and became the main contact between Romansy and CISM. Also, the incredibly efficient Mrs. Bertozzi was also still available. After the symposium, Professors McGhee, Thring and Warnecke left the committee, and Prof. Morecki became the chairman of the CISM-IFTToMM Technical Committee on Robots and Manipulators. Prof. Bianchi became the vice chairman. The fifth Romansy was back at CISM and, accordingly, Bianchi and Morecki had switched chairman and vice chairman roles.

The sixth was back in Poland on September 9–12, 1986. This time the venue was in the city of Krakow. The symposium opened with a memorial session dedicated to the work of Jean Vertut, who had died of a heart attack at age 56. After the sixth Kato, Kobrinskii, Kędzior and I left the Organizing and Program Committee. For me, it was time to let the next generation pilot the Romansy voyage.

7 Conclusions

When Romansy was started it was the first research based conferences dealing with robot design, mechanics and control. Furthermore, before Romansy there was little or no interchange between Eastern Europe and the West on these subjects. Romansy was created on the premise of free scientific communication between all areas of the world. The fact that it achieved its original goals and continues to thrive is of great personal satisfaction to me. Even greater satisfaction for me is the great gift of the enduring and cherished friendships formed through Romansy.

Parametric Method for Motion Analysis of Manipulators with Uncertainty in Kinematic Parameters

Vahid Nazari and Leila Notash

Abstract In this paper, the motion performance of manipulators considering the uncertainty in the kinematic parameters is investigated. Interval analysis is employed to deal with the uncertainty in the kinematic parameters in the form of small uncertainty boxes. For a given range of uncertainties in the kinematic parameters, the interval linear equations are formulated to relate the velocity of joints to the end effector velocity with the Jacobian matrix. A novel approach for calculating the exact size and shape of the solution for the system of interval linear equations is presented. A 2 degrees of freedom planar serial manipulator is used as a case study to analyze the motion performance of the manipulator in the presence of uncertainties.

Keywords Interval analysis · Robot manipulators · Uncertainty · Parametric method · Parameter solution set

1 Introduction

Robot manipulators are typical of systems that are intrinsically subjected to uncertainties. The nominal relationship between the end effector pose and joints displacement is known but this relationship is not necessarily accurate due to changes in the robot hardware and uncertainties in the kinematic parameters [1]. A real robot analysis should be performed in the presence of uncertainties in the

V. Nazari (✉) · L. Notash
Department of Mechanical and Materials Engineering, Queen's University, Kingston,
Canada
e-mail: nazariv@me.queensu.ca

L. Notash
e-mail: notash@me.queensu.ca

modeling of the manipulator and measurements of the kinematic parameters. The sources of uncertainties include the manufacturing tolerances of the mechanical parts, measurement error, control error, and round-off error. All types of uncertainties can be accommodated as bounded variations in the kinematic parameters.

Several methods are known for calculating the lower and upper bounds for each component of the solution set in the interval linear systems. One of the first contributions on determining the bounds of the solution set was given in [2]. It was shown that the solution set for this system is a polyhedron. More general algorithms for determining the bounds containing the exact solution were presented in [3–5]. These bounds were not necessarily identical to the exact solution. The exact solution was determined in [6] as the union of finitely many convex polytopes whose vertices were denoted by matrices with entries equal to the lower or upper bounds of the interval coefficient matrix. The shape of the solution set, in general, was a non-convex polyhedron.

The exact solution of the interval linear systems is generally complicated and not easily described. Therefore, calculation of this solution is computationally expensive and, hence, is not convenient to use for the real time application. Accordingly, the researchers are drawn to find the fastest methods to enclose the exact solution. One of the first publications on parametric interval systems for special coefficient matrices, such as symmetric and skew-symmetric matrices, was presented in [7, 8]. The characterization of the boundary of the solution set of the parametric system based on a set of inequalities was done by [9]. This approach was designed particularly for visualizing the boundary of the parametric solution set.

In this paper, the motion performance of manipulators with uncertainty in the kinematic parameters is investigated using parametric interval method. The organization of paper is as follows. The basic principles of the interval analysis and the parametric interval systems are given in Sect. 2. The proposed methodology for formulating the exact solution, which is based on parameterizing the interval linear systems, is presented in Sect. 3. The simulation results are reported in Sect. 4 and the paper is concluded in Sect. 5.

2 Parametric System of Interval Linear Equations

Interval analysis is a numerical method of representing the uncertainty in values by replacing a number with a finite range of values. An interval denoted by $[X] = [\underline{X}, \overline{X}]$ is the set of real numbers X verifying $\underline{X} \leq X \leq \overline{X}$ where \underline{X} and \overline{X} are the lower and upper bounds of the interval, respectively. The interval is also represented by the midpoint, X_c , and the radius, ΔX , as $[X] = [X_c - \Delta X, X_c + \Delta X]$ or $[X] = X_c + \Delta X[-1, 1]$. A real number is a special case of an interval in which $\underline{X} = \overline{X}$. The width of the interval $[X]$ is defined as $w(X) = \overline{X} - \underline{X}$. The midpoint of $[X]$ is given by $m(X) = \frac{1}{2}(\overline{X} + \underline{X})$. A matrix whose entries are interval is called an interval matrix and denoted by $[A]$, A_c , is the midpoint of $[A]$ whose entries are the

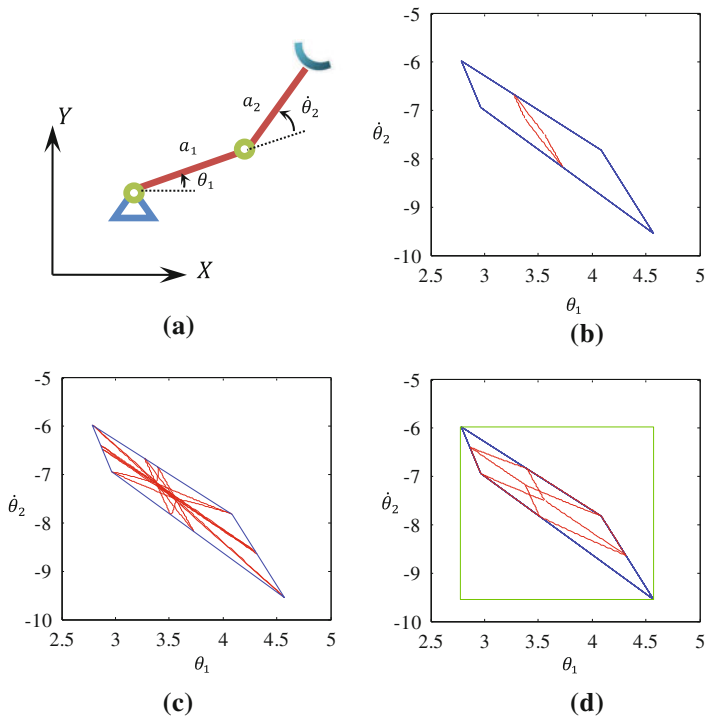


Fig. 1 **a** 2 DOF planar serial manipulator, **b** one of two-parameter solution sets in *red*, **c** all two-parameter solution sets in *red* and the exact solution in *blue*, **d** a three-parameter solution set in *red* and the smallest box containing the exact solution in *green*

midpoints of the corresponding entries of $[\mathbf{A}]$, the radius of the interval matrix, Δ , is defined as $\frac{1}{2}(\overline{\mathbf{A}} - \underline{\mathbf{A}})$.

In manipulators, the Jacobian matrix relates the joint velocity vector to the end effector velocity vector. Due to the uncertainty in the kinematic parameters, the relationship between the joint velocity vector and the end effector velocity vector takes the form of the interval linear system. This interval system is parameterized as $[\mathbf{J}([\mathbf{p}]])\dot{\mathbf{q}} = [\mathbf{V}([\mathbf{p}])]$ in which the entries of the Jacobian matrix and the end effector velocity vector linearly depend on parameters $[\mathbf{p}] = ([p_1], [p_2], \dots, [p_K])$ even though in general, the entries of the Jacobian matrix and the velocity vector could be nonlinear functions of the interval parameters $[\mathbf{p}]$. The exact values of these parameters are unknown but bounded within given intervals. Considering the serial manipulator in Fig. 1a and using a linear parametric model for each entry of $[\mathbf{J}([\mathbf{p}])]$ and $[\mathbf{V}([\mathbf{p}])]$, the entries of the Jacobian matrix and the velocity vector could be defined as

$$[J_{jk}(\mathbf{p})] = J_{jk,0} + \sum_{\mu=1}^K J_{jk,\mu} [p_{\mu}], [V_j(\mathbf{p})] = V_{j,0} + \sum_{\mu=1}^K V_{j,\mu} [p_{\mu}] \quad (1)$$

where $J_{jk,\mu}, V_{j,\mu} \in \mathbb{R}$; $\mu = 1, \dots, k; j = 1, \dots, m; k = 1, \dots, n$; m is the task space dimension and n is the number of joints. The value of parameter K depends on the number of the interval parameters used to parameterize the interval system. The maximum number of the interval entries of $[\mathbf{J}]$ and $[\mathbf{V}]$ is mn and m , respectively. Depending on the uncertainty of the kinematic parameters in the manipulator, some entries of the Jacobian matrix and the end effector velocity vector may not be interval.

3 Parametric Method for Exact Solution

In this section, the exact solution of the interval system is calculated using solution sets obtained from parameter groups of interval systems. Depending on the number of interval parameters involved in the Jacobian matrix and the velocity vector, the exact solution will be characterized. The parameter assignment of the entries of $[\mathbf{J}]$ and $[\mathbf{V}]$ in the manipulator is performed by selecting some interval entries of either $[\mathbf{J}]$ or $[\mathbf{V}]$ as parameters $[p_{\mu}]$ and formulating other entries as functions of interval parameters $[p_{\mu}]$. All parameter assignments of the entries of $[\mathbf{J}]$ and $[\mathbf{V}]$ which lead to the same solution set are collected as one parameter group. That is, a parameter group may consist of one or several different parameter assignments.

The number of parameter groups in each interval system depends on the total number of interval entries of $[\mathbf{J}(\mathbf{p})]$ and $[\mathbf{V}(\mathbf{p})]$, denoted as η , and the number of interval parameters in the interval system, K . The solution sets of all parameter assignments of the interval system are checked and the parameter assignments which result in the same solution set are categorized as one parameter group. Considering a general spatial serial manipulator, to form $[\mathbf{J}] \dot{\mathbf{q}} = [\mathbf{V}]$ with η interval entries in $[\mathbf{J}]$ and $[\mathbf{V}]$ and 2 interval parameters, $K = 2$, there exist $\frac{1}{2} \sum_{i=K-1}^{\eta-1} \binom{\eta}{i} = \frac{1}{2} \sum_{i=1}^{\eta-1} \frac{\eta!}{(\eta-i)!i!}$ different parameter groups. When the number of interval parameters is $K = 3$, all the number of possible parameter groups is

$$\text{calculated as } \sum_{i=K-1}^{\eta-2} \frac{\binom{\eta}{i} \binom{\eta-i}{2}}{(\eta-i-2)!} = \sum_{i=2}^{\eta-2} \frac{(\eta-i-1)(\eta-i)\dots(\eta)}{2!i!(\eta-i-2)!}.$$

In this paper, once the numerical interval matrix $[\mathbf{J}]$ is calculated, the entries of $[\mathbf{J}(\mathbf{p})]$ and $[\mathbf{V}(\mathbf{p})]$ are expressed as linear functions of the interval parameters $[p_{\mu}]$, $1 \leq \mu \leq K$. Considering entry $[J_{jk}]$ and $[V_j]$ as linear function of $[p_{\mu}]$, then $[J_{jk}([p_{\mu}])] = J_{jk,0} + J_{jk,\mu}[p_{\mu}]$ and $[V_j(p_{\mu})] = V_{j,0} + V_{j,\mu}[p_{\mu}]$. The lower and upper bounds of any interval entry $[J_{jk}] = [\underline{J}_{jk}, \overline{J}_{jk}]$ are related to those of interval parameter $p_{\mu} \in [p_{\mu}, \overline{p}_{\mu}]$, $p_{\mu} \neq \overline{p}_{\mu}$ through the following system of linear equations

$$\begin{cases} \overline{J_{jk}} = J_{jk,0}\overline{p}_\mu + J_{jk,\mu} \\ \underline{J_{jk}} = J_{jk,0}\underline{p}_\mu + J_{jk,\mu} \end{cases} \Rightarrow \begin{bmatrix} \overline{p}_\mu & 1 \\ \underline{p}_\mu & 1 \end{bmatrix} \begin{bmatrix} J_{jk,0} \\ J_{jk,\mu} \end{bmatrix} = \begin{bmatrix} \overline{J_{jk}} \\ \underline{J_{jk}} \end{bmatrix} \quad (2)$$

The coefficients ${}^i J_{jk,0}$ and ${}^i J_{jk,\mu}$ are calculated by taking inverse of Eq. (2) as

$$\begin{bmatrix} J_{jk,0} \\ J_{jk,\mu} \end{bmatrix} = \begin{bmatrix} \overline{p}_\mu & 1 \\ \underline{p}_\mu & 1 \end{bmatrix}^{-1} \begin{bmatrix} \overline{J_{jk}} \\ \underline{J_{jk}} \end{bmatrix} \quad (3)$$

The same procedure is performed to formulate the entry of $[V_j]$ as a function of $[p_\mu]$. It should be noted that the entry of $[\mathbf{J}([\mathbf{p}]])$ or $[\mathbf{V}([\mathbf{p}]])$ nominated for the interval parameter must be interval. Otherwise, the matrix in Eq. (2) would be singular and the entry $[J_{jk}]$ cannot be formulated in terms of parameter $[p_\mu]$. If $[\mathbf{J}([\mathbf{p}]])$ is an $n \times n$ square matrix and non-singular for each $p_\mu \in [\underline{p}_\mu, \overline{p}_\mu]$, $\mu = 1, \dots, K$, $[\mathbf{J}^{-1}([\mathbf{p}]])$ exists and $[\dot{\mathbf{q}}([\mathbf{p}]]) = [\mathbf{J}^{-1}([\mathbf{p}]])[\mathbf{V}([\mathbf{p}]])$ is a function of K interval parameters which is continuous [9]. This parametric joint velocity vector provides the solution set for each parameter group.

When the parametric Jacobian matrix is of full-rank, the solution which minimizes the 2-norm of the joint velocity vector is selected. If the square parametric matrix $[\mathbf{J}([\mathbf{p}]])[\mathbf{J}^T([\mathbf{p}]])$ is regular for every $p_\mu \in [\underline{p}_\mu, \overline{p}_\mu]$, the minimum 2-norm solution set to the parametric system exists and is formulated as a function of interval parameters $[\dot{\mathbf{q}}([\mathbf{p}]]) = [\mathbf{J}^T([\mathbf{p}]])([\mathbf{J}([\mathbf{p}]])[\mathbf{J}^T([\mathbf{p}]])^{-1}[\mathbf{V}([\mathbf{p}]])]$. If the manipulator has a combination of revolute and prismatic joints, the joint velocity vector is not physically consistent. If the interval entries with the same dimension are parameterized, a weighting matrix would be required to calculate the generalized (Moore-Penrose) inverse of $[\mathbf{J}([\mathbf{p}]])$ as $\mathbf{J}^\# = \mathbf{W}[\mathbf{J}^T([\mathbf{p}]])([\mathbf{J}([\mathbf{p}]])\mathbf{W}[\mathbf{J}^T([\mathbf{p}]])^{-1}]$.

Similarly, when parametric Jacobian matrix $[\mathbf{J}([\mathbf{p}]])$ is of full column-rank and $[\mathbf{J}^T([\mathbf{p}]])[\mathbf{J}([\mathbf{p}]])$ is regular for every $p_\mu \in [\underline{p}_\mu, \overline{p}_\mu]$, the least square solution set is calculated. The weighted left generalized inverse of $[\mathbf{J}([\mathbf{p}]])$ is calculated as $\mathbf{J}^\# = [\mathbf{J}^T([\mathbf{p}])\mathbf{W}[\mathbf{J}([\mathbf{p}]])^{-1}\mathbf{J}([\mathbf{p}])\mathbf{W}]$ if the interval entries of the Jacobian matrix are parameterized using the interval parameters with the same dimension.

4 Case Study

In this section, the 2 DOF planar serial manipulator in Fig. 1a with two revolute joints is used as a case study for the interval analysis to visualize the solution set. The manipulator has uncertainty in two joint variables θ_1 and θ_2 and the link lengths a_1 and a_2 .

For the joint variables $\theta_1 = \frac{\pi}{6}$ rad and $\theta_2 = \frac{\pi}{4}$ rad, the link lengths $a_1 = a_2 = 0.5$ m, the radius of uncertainty $\frac{\pi}{180}$ rad in θ_1 and θ_2 and the radius of

uncertainty 0.010 m in link lengths, the interval Jacobian matrix is $\mathbf{J} = \begin{pmatrix} [-0.760, -0.706] & [-0.497, -0.469] \\ [0.530, 0.595] & [0.110, 0.149] \end{pmatrix}$. The desired end effector velocity is $\mathbf{V} = [v_x v_y]^T = [1 \ 1]^T$ (m/s).

If the Jacobian matrix and the end effector velocity vector are functions of two parameters $[p_1]$ and $[p_2]$, i.e., $\mu = 1, 2$, the parametric linear system will be

$$\mathbf{J}([\mathbf{p}]) \begin{bmatrix} \dot{\theta}_1 \\ \dot{\theta}_2 \end{bmatrix} = \begin{pmatrix} [v_x([\mathbf{p})]] \\ [v_y([\mathbf{p})]] \end{pmatrix} \quad (4)$$

The parameter solution set is derived using the inverse of $\mathbf{J}([\mathbf{p}])$ as

$$\dot{\theta}([\mathbf{p}]) = \begin{pmatrix} [\dot{\theta}_1([\mathbf{p})]] \\ [\dot{\theta}_2([\mathbf{p})]] \end{pmatrix} = \mathbf{J}([\mathbf{p}])^{-1} \begin{pmatrix} [v_x([\mathbf{p})]] \\ [v_y([\mathbf{p})]] \end{pmatrix} \quad (5)$$

Generally, the entries of the Jacobian matrix and the end effector velocity vector can be parameterized such that the entries with the consistent dimension are categorized in the same groups. In this example, the Jacobian matrix has physically consistent entries. Therefore, the parameter assignment can be performed to any entries of the Jacobian matrix. If the entries of the end effector velocity vector are interval and have the same dimension, e.g., m/s, these entries could be parameterized using an interval parameter with the same dimension, e.g., m/s. In the case study, the entries of the end effector velocity vector are not interval. Therefore, they are not functions of an interval parameter, i.e., $[V_j] = V_{j,0} = 1$, $j = 1, 2$.

Entries $[J_{12}]$ and $[J_{11}]$ are selected as the interval parameters $p_1 \in [-0.497, -0.469]$ and $p_2 \in [-0.760, -0.706]$, entries $[J_{21}]$ and $[J_{22}]$ are assigned as functions of $[p_1]$ and entries v_x and v_y are constant values 1. The interval entries of Eq. (3) are substituted into Eq. (5) and the two-parameter solution set for this parameter group is formulated as

$$\dot{\theta}(p_1, p_2) = \begin{pmatrix} \frac{-0.372[p_1] - 0.792}{1.669[p_1] - 0.792[p_2] - 1.372[p_1][p_2] + 2.291[p_1]^2} \\ \frac{2.291[p_1] - [p_2] + 1.669}{1.669[p_1] - 0.792[p_2] - 1.372[p_1][p_2] + 2.291[p_1]^2} \end{pmatrix} \quad (6)$$

Similar to the procedure in calculating the two-parameter solution set in Eq. (6), the two-parameter solution set for each parameter group is formulated. Other parameter groups are obtained by new parameter assignment of the interval entries of $\mathbf{J}([\mathbf{p}])$ as either $[p_1]$ or $[p_2]$ and the rest of entries as functions of $[p_1]$ and $[p_2]$. The new parameter solution set for each parameter assignment forms a parameter group. The boundary curves of the solution set for each group of parametric linear system are specified by 4 curves; two curves $\dot{\theta}(p_1, \underline{p}_2)$ and $\dot{\theta}(p_1, \bar{p}_2)$ in 2-dimensional space when p_1 varies from \underline{p}_1 to \bar{p}_1 and p_2 is set once to

the lower bound and then to the upper bound. Similarly, the other two curves $\dot{\theta}(p_2, p_1)$ and $\dot{\theta}(p_2, \bar{p}_1)$ are formulated when p_2 varies from \underline{p}_2 to \bar{p}_2 and p_1 is set to the lower bound and the upper bound, respectively. In the resulting solution set enclosed by four curves, each curve is connected to the other two curves in two points and the two attached curves share a point. Therefore, four points $\dot{\theta}(\underline{p}_1, \underline{p}_2)$, $\dot{\theta}(\bar{p}_1, \bar{p}_2)$, $\dot{\theta}(\underline{p}_1, \bar{p}_2)$ and $\dot{\theta}(\bar{p}_1, \underline{p}_2)$ form vertices of the solution set for each parameter group. This two-parameter solution set (in red color) is illustrated in Fig. 1b and completely lies inside the exact solution (in blue color).

To characterize the exact solution, first all parameter groups which result in the same solution sets are determined and then plotted in $\dot{\theta}_1$ - $\dot{\theta}_2$ plane. In this example, since there are four interval entries in the Jacobian matrix, $\eta = 4$, there will exist $\frac{1}{2} \sum_{i=1}^{\eta-1} \frac{\eta!}{(\eta-i)!i!} = \frac{1}{2} \sum_{i=1}^3 \frac{4!}{(4-i)!i!} = \frac{1}{2} (4 + 6 + 4) = 7$ different parameter groups among all possible solution sets, i.e., $2^4 = 16$. These 16 solution sets are illustrated in red color in Fig. 1c. The outer vertices of the different groups of the two-parameter solution sets are connected to form the boundary of the exact solution (in blue color). Generally speaking, when the exact solution is non-convex, the two-parameter solution sets might not be able to distinguish the indented vertices.

In the three-parameter case, each parameter group includes interval parameters $[p_1]$, $[p_2]$ and $[p_3]$, i.e., $\mu = 1, 2, 3$. The procedure to calculate the solution set for each parameter group is similar to that of the two-parameter case. The parameter groups for three interval parameters are $\sum_{i=2}^{\eta-2} \frac{(4-i-1)(4-i)\dots(4)}{2!i!(4-i-2)!} = 6$. The solution set corresponding to each parameter group consists of 12 curves; the two parameters p_1, p_2 are set to either lower or upper bounds and the resulting 4 curves, which are functions of parameter p_3 , are plotted when p_3 varies within the lower and upper bounds. The formulation of the solution set of the interval system including three parameters is applicable to the Jacobian matrices of the manipulators with more than 2 joints such as planar 3 DOF manipulators. The process is repeated when $[p_1], [p_3]$ are set to either the lower or upper bounds and the next 4 curves are functions of $[p_2]$. The last 4 curves are formulated as functions of $[p_1]$ when $[p_2], [p_3]$ are set to either the lower or upper bounds. The resulting 12 curves form a hypersurface which may have surfaces on the boundary surface of the exact solution.

To show the solution set for a group of parametric linear system with three interval parameters, the same example as the two-parameter case is considered. For entries $[J_{11}]$ and $[J_{12}]$ and $[J_{21}]$ as interval parameters $p_1 \in [-0.760, -0.706]$, $p_2 \in [-0.497, -0.469]$ and $p_3 \in [0.530, 0.595]$, respectively, $[J_{22}]$ as a function of $[p_1]$, and $[v_x]$ and $[v_y]$ as constant values, the three-parameter solution set is plotted in Fig. 1d. As illustrated, some edges of this solution set lie on the boundary of the exact solution. The commonly calculated smallest box containing the exact solution is depicted in Fig. 1d in green color. As shown, this solution is much larger than the exact solution.

In general, for K -parameter case, the number of curves involved to form the solution set of each parameter group is calculated to be $K \times 2^{(K-1)}$. For instance, in three-parameter case, the number of curves which forms the solution set for each parameter group is $3 \times 2^2 = 12$. It should be noted that as the size of the interval matrix, especially the interval entries of the matrix, increases, the total number of the parameter groups which have different solution sets drastically grows.

The drawback of the two-parameter solution set is that the indented vertices of the exact solution, if there is any, may be ignored. The three-parameter solution set overcomes this limitation as more curves are contributed to characterize each three-parameter solution set, and hence the actual vertices of the exact solution set are obtained. The interval analysis in this paper is performed using INTLAB [10].

5 Discussion and Conclusions

In this paper, the motion analysis of manipulators considering uncertainty in the kinematic parameters were investigated, and a novel method to identify the exact solution of joint velocities for the given end effector velocities was presented. To model the uncertainty in kinematic parameters, interval analysis was applied and the lower and upper bounds of each entry of the Jacobian matrix were determined and the interval linear equations were formulated to relate the velocity of joints to the end effector velocity. Although the range of uncertainties in the kinematic parameters was small, the accumulation effect of uncertainties caused a relatively wide solution for the velocity of the joints. The lower and upper bounds of the joint velocity components depended on the length of the links, the range of uncertainties and the configuration of the manipulator. When the manipulator is close to the singular configuration, even for small values of uncertainties, the width of joint velocity components increases. The proposed method has been implemented for the serial and parallel manipulators. Due to space limitation, only the results for a serial manipulator were reported here.

Generally, there is a trade-off between the accuracy of the solution and the computation time. The parametric interval system provides the exact solution with more computation effort. For offline analysis such as the investigation of workspace of manipulators, since the calculation time is not a concern, the parametric interval method is valuable. In real time applications, methods that are not computationally expensive are better suited. As a future work, the motion analysis of manipulators with uncertainty in the kinematic parameters, velocity limits of the joints and the joint failure will be investigated.

References

1. Roth, Z., Mooring, B., Ravani, B.: An overview of robot calibration. *IEEE J. Robot. Autom.* **3**, 377–385 (1987)
2. Oettli, W.: On the solution set of a linear system with inaccurate coefficients. *J. Soc. Ind. Appl. Math. Series B. Numer. Anal.* **2**, 115–118 (1965)
3. Hansen, E., Smith, R.: Interval arithmetic in matrix computations, part II. *SIAM J. Numer. Anal.* **4**, 1–9 (1967)
4. Neumaier, A.: *Interval Methods for Systems of Equations*. Cambridge University Press, Cambridge (1990)
5. Oettli, W., Prager, W., Wilkinson, J.: Admissible solutions of linear systems with not sharply defined coefficients. *J. Soc. Ind. Appl. Math. Series B. Numer. Anal.* **2**, 291–299 (1965)
6. Hartfiel, D.: Concerning the solution set of $Ax = b$ where $P \leq A \leq Q$ and $p \leq b \leq q$. *Numer. Math.* **35**, 355–359 (1980)
7. Jansson, C.: Interval linear systems with symmetric matrices, skew-symmetric matrices and dependencies in the right hand side. *Computing* **46**, 265–274 (1991)
8. Alefeld, G., Kreinovich, V., Mayer, G.: On the shape of the symmetric, persymmetric, and skew-symmetric solution set. *SIAM J. Matrix Anal. Appl.* **18**, 693–705 (1997)
9. Popova, E., Krämer, W.: Visualizing parametric solution sets. *BIT Numer. Math.* **48**, 95–115 (2008)
10. Rump, S.M.: INTLAB: INTerval LABoratory. In: Csendes, T. (ed.) *Developments in Reliable Computing*, pp. 77–104. Kluwer Academic Publishers, Dordrecht (1999)

Self-Adjusting Isostatic Exoskeleton for the Elbow Joint: Mechanical Design

V. A. Dung Cai and Philippe Bidaud

Abstract This paper describes the mechanical design of an active orthosis device for the human elbow joint. The device can be used in muscle stretching application to help the patient's elbow recovering its full range of motion after surgery intervention. We use a 6 degree of freedom mechanism, including an 4D parallel Delta type mechanism, to assure that the motor torque can be fully transmitted to the anatomical axis of the elbow without creating residual efforts that may limit the natural motion of the joint.

Keywords Orthosis devices • Parallel manipulators • Design • Experimental tests

1 Introduction

1.1 Related Work

Recent works on the design of exoskeletons for human anatomical joint have figured out the importance of the use of passive joints in the device's mechanism so that the whole mechanical chain will become isostatic when it is attached to the human corporel segments. Indeed, a human anatomical joint is in most cases

V. A. Dung Cai (✉)

Faculty of Mechanical Engineering, University of Technical Education,
01 Vo Van Ngan Street, Thu Duc District, Ho Chi Minh City, Vietnam
e-mail: dungcva@hcmute.edu.vn

P. Bidaud

Institut des Systèmes Intelligents et de Robotique, UPMC University Paris 06,
4 Place Jussieu, 75005 Paris, France
e-mail: bidaud@isir.upmc.fr

spatial and can not be reduced to simple elementary mechanical joints [1, 2, 9, 10]. Thus, the design of exoskeletons for functional rehabilitation must take into account the complexity of anatomical joints. A misalignment between the instantaneous anatomical axis and the actuated axis of the mechanism will create residual efforts that may limit natural motion of the joint, or even cause permanent injuries in extreme cases.

In 2006, Schiele and Van der Helm [8] presented a novel design for human arm exoskeleton which has 9 d.o.f. in total. In this design, a RPR mechanism is used at the elbow joint. Only the first rotational joint is actuated while the two other joints are passive, assuring that only the actuator torque will be transmitted to the elbow. It was followed by different original designs in literature such as [3, 5, 7, 9]. Later in 2011, Cai et al. [3] established a general design rule for exoskeletons that can be summarized as follow:

- The mechanism must have at least 3 d.o.f. in the case of planar anatomical joint. It must have at least 6 d.o.f. in the case of spatial anatomical joint.
- The number of passive joints used in the mechanism is equal to the difference between the space dimension (3 or 6) and the mobility of the anatomical joint.
- The number of actuators is the difference between the degree of freedom of the mechanism and the number of passive joints.
- Generally, for passive rehabilitation exercises, the mechanism must be designed adequately so that it can mobilize the anatomical joint in flexion or in extension by transmitting opposing torques on the two limbs of the subject. The transmitting torque orientation must be close to the that of the human anatomical axis. All other force and torque components must be minimized.

1.2 Elbow Exoskeleton

The design proposed by Schiele and Van der Helm [8] did not take into account the fact that the elbow joint, formed by the humero-ulna joint, the humero-radial joint and the proximal radio-ulna joint, is a complex spatial joint which might not be modeled by a simple serial mechanism with 2 rotation joints representing the flexion/extension and the forehand axial rotation (supination/pronation). Bottlang et al. and Ericson et al. [1, 6] figured out that the elbow kinematic should be modeled by a screw displacement axis which allow the representation of all anatomical kinematic data, which are flexion/extension, valgus/varus angles and proximal/distal, anterior/posterior displacement.

This paper describes a novel design of an active orthosis for the passive rehabilitation of elbow joint. The device kinematics is equivalent to a 3R-3P mechanism which is quasi-isotropic. The use of a Delta-type parallel mechanism not only allows the substitution of the 3 prismatic joints by bearing joints but also gives the mechanism a better torque transmission capability by its symmetric structure.

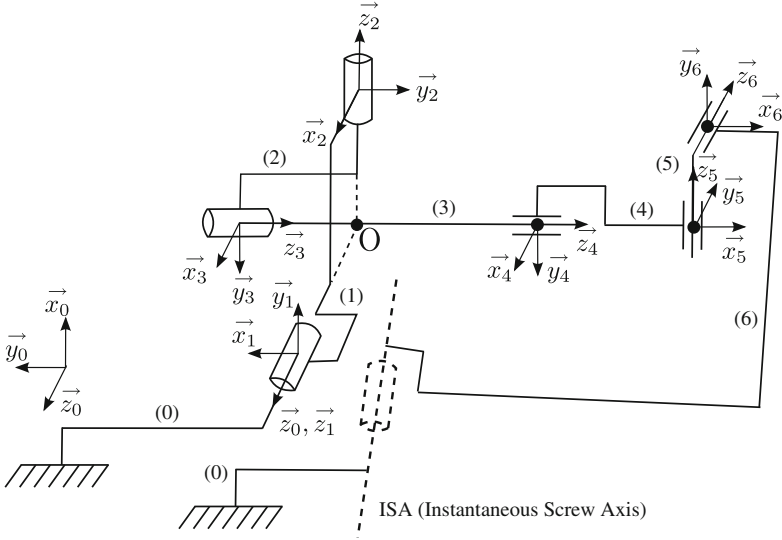


Fig. 1 Frame assignment of a 3R-3P mechanism

2 Isotropic Property

According to Chablat and Angeles [4], isotropy is always sought in the mechanical design of manipulators because it increases the robustness of the assembly and measurement errors. Isotropy also assure uniform force transmission capability, and for this reason, designers should try to use isotropic mechanisms in the design of active rehabilitation devices. Cai et al. [3] presented a knee exoskeleton with 6 d.o.f. RRRPRR mechanism which has a conditioning number around 3. However, the most commonly used mechanism is 3R-3P (A serial mechanism which includes 3 intersecting rotary joints and 3 prismatic joint). It is possible to demonstrate that the condition number of the latter is close to 1.

The Fig. 1 represents the kinematic model of a 3R-3P mechanism. By definition, the conditioning number of a matrix can be defined by the ratio between the largest and smallest singular values, which are the square roots of the eigenvalues of the positive semi-definite matrix JJ^t . In this case we have a matrix J homogeneous in dimension. Thus the computation of JJ^t yields:

$$JJ^t / R_2 = \begin{pmatrix} \cos^2 \theta_2 & -\sin \theta_2 \cos \theta_2 & 0 & 0 & 0 & 0 \\ -\sin \theta_2 \cos \theta_2 & \sin^2 \theta_2 + 1 & 0 & 0 & 0 & 0 \\ 0 & 0 & 1 & 0 & 0 & 0 \\ 0 & 0 & 0 & 1 & 0 & 0 \\ 0 & 0 & 0 & 0 & 1 & 0 \\ 0 & 0 & 0 & 0 & 0 & 1 \end{pmatrix}. \quad (1)$$

The eigenvalues of the matrix \mathbf{JJ}^t are the roots its characteristic polynomial, which can be determined by:

$$\begin{aligned}
 P(X)_{\mathbf{JJ}^t} &= \det \begin{vmatrix} \cos^2 \theta_2 - X & -\sin \theta_2 \cos \theta_2 & 0 & 0 & 0 & 0 \\ -\sin \theta_2 \cos \theta_2 & \sin^2 \theta_2 + 1 - X & 0 & 0 & 0 & 0 \\ 0 & 0 & 1 - X & 0 & 0 & 0 \\ 0 & 0 & 0 & 1 - X & 0 & 0 \\ 0 & 0 & 0 & 0 & 1 - X & 0 \\ 0 & 0 & 0 & 0 & 0 & 1 - X \end{vmatrix} \\
 &= \det \begin{vmatrix} \cos^2 \theta_2 - X & -\sin \theta_2 \cos \theta_2 & 0 \\ -\sin \theta_2 \cos \theta_2 & \sin^2 \theta_2 + 1 - X & 0 \\ 0 & 0 & 1 - X \end{vmatrix} \cdot \det \begin{vmatrix} 1 - X & 0 & 0 \\ 0 & 1 - X & 0 \\ 0 & 0 & 1 - X \end{vmatrix} \\
 &= (1 - X)^4 (X^2 - 2X + \cos^2 \theta_2).
 \end{aligned} \tag{2}$$

The eigenvalues of the matrix \mathbf{JJ}^t are thus:

$$\begin{cases} X = 1, \\ X = 1 \pm |\sin \theta_2| \end{cases} \tag{3}$$

Therefore we can obtain the conditioning number of the mechanism as follow:

$$K = \sqrt{\frac{1}{1 - |\sin \theta_2|}} \tag{4}$$

where θ_2 represents the varus/valgus angular position, which is limited to 20° here. Consequently, the maximum conditioning number of the mechanism is 1.23. The mechanism is thus quasi-isotropic.

3 Mechanical Design

3.1 Kinematic Choice

Beside the quasi-isotropic property, The 3R-3P mechanism also allows the decoupling of torques and the forces, then pure torques can be transmitted to the human anatomical joint, without any linear force components which may cause sliding movements of the attaches. However, the use of prismatic joints is usually not suitable due to their massive weight and expensive cost. Then replacement mechanisms, composed by parallelograms, using only bearing joints should be considered. For that purpose, we proposed the use of Delta type parallel mechanism to substitute the 3 prismatic joints.

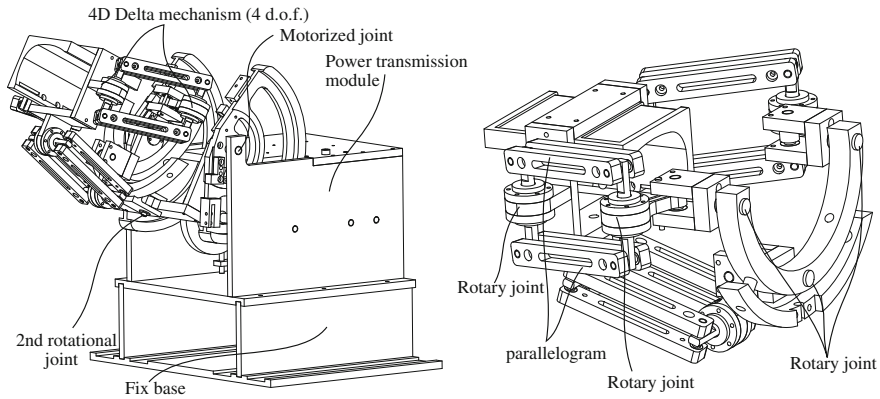


Fig. 2 **a** 3D computer model of the device. **b** The 4 d.o.f. delta type linkage: the close-loop mechanism is composed by 3 chains, each chain is a R-R-Pa-R mechanism

The proposed mechanism in this paper is a hybrid structure composed by 2 rotational joints in series with a 4D Delta parallel mechanism, forming a 6 degrees of freedom mechanism. With this design, the motor torque will be transmitted in the sagittal plane of the elbow, thus assuring the stability of the whole system.

3.2 Description of the Design

Figure 2 show the details of the mechanical linkage of the device. The 4D Delta type parallel linkage is composed by 3 chains. Each chain is formed by 3 rotary joints in series with a parallelogram that connects to the extremity base through a 4th rotary joint (which can be called here a R-R-R-Pa-R mechanism). The 3 first rotary joint added at each chain allow to free an additional rotational degree of freedom for the 4D Delta linkage, besides the 3 other degrees of freedom in translation. The virtual axis of rotation of this 4th degree of freedom is located near to the that of the forearm, thus allowing the elbow supination/pronation movement.

Figure 3 illustrates the transmission module. The device can provide a torque of 20 Nm through the use of a DC motor and a three-stage, backdrivable, 120:1 transmission. It comprises two high-speed friction drives followed by a low speed cable-drive. The 2nd and the 3rd stage give a torque gain 10 and 12 respectively.

The first friction drive operates through direct contact between the surface of a disk (directly fixed to the motor shaft) and 2 disk drives (of type cylinder—elastic half space contact). The elasticity is regulated by 4 compression springs pushing on the motor disk. The second friction drive is of type contact between two cylinders with parallel axes. For this 2nd stage, contact is regulated by a compression spring pushing on rollers so that slip does not occur. These systems allow the adjustment the threshold of slipping, and thus provides an extra level of safety for users.

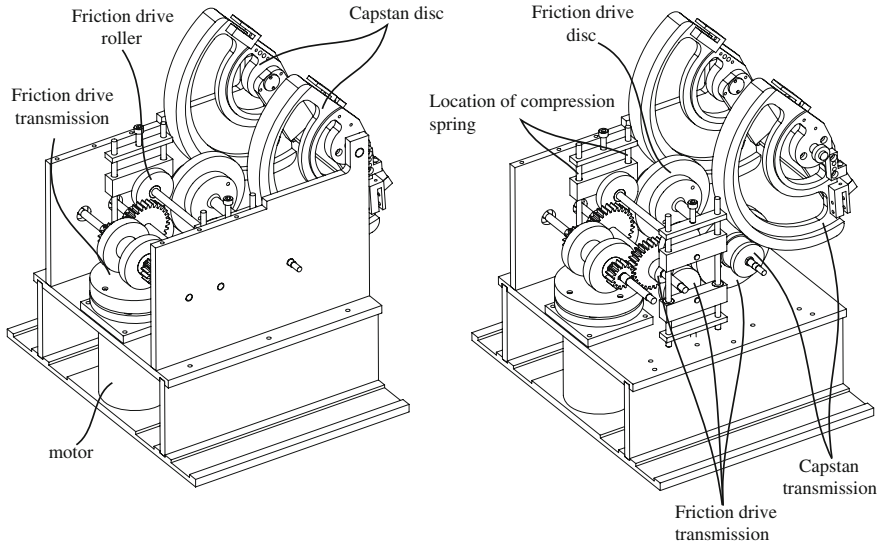


Fig. 3 The transmission module with a power ratio of 120:1

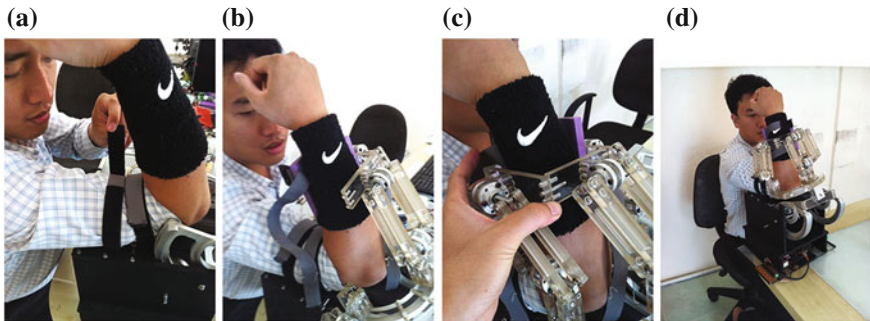


Fig. 4 Set up protocol to attach the device to the subject's limbs. **a** The subject's arm is being attached to the fixed base. **b** The forearm is being attached to the mechanism, the third mechanical chain is detached. **c** The third mechanical chain is re-attached to the mechanism. **d** End of set up protocol, the system is ready to use

4 Result

The first version of the device was manufactured, assembled and tested. Figure 4 shows the set up protocol on the user's arm. As the device is designed for muscular stretching exercises with patient having flexed elbow then the protocol must begin at full flexion. One of the 3 mechanical chains is detached at the beginning so that the rehabilitation practitioner can attach the mechanism to the user's forearm. This chain will be re-attached to the mechanism once the forearm is firmly in place.

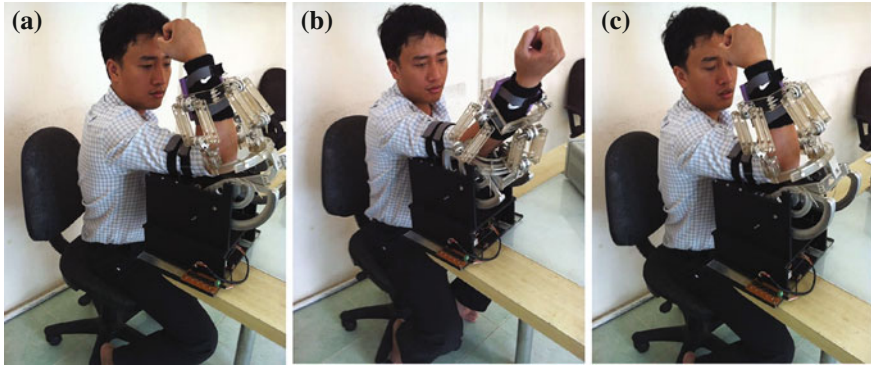


Fig. 5 Elbow stretching exercise. **a** The beginning of the exercise. **b** The device pull the elbows to a predefined position. **c** The torque set-point is set to zero, then the elbow joint can return to its initial position due to its stiffness

Preliminary results are satisfactory. We used a current sensor to monitor the motor torque and an optical encoder to measure the flexion angular position. The following algorithm was implemented for our very first experiments:

- 1st step: Pull the elbow to a certain predefined angle. The torque is controlled so that the user elbow can oscillate around this angular position.
- 2nd step: Let the elbow return to full-flexion by setting the torque set-point to zero.
- Return to the 1st step to repeat the exercise (Fig. 5).

5 Conclusion

In this paper, we presented an isostatic 6 d.o.f active orthosis device for the elbow joint. The device is composed by 2 rotational joints and a 4D Delta-type parallel mechanical linkage, assuring the stability of the whole system and keeping the mechanism's conditioning number near to 1. The first rotational joint is actuated, transmitting the motor torque to the forearm to drive the elbow in flexion-extension. Friction drive and cable drive are used to provide a safe, back-driven and high ratio mechanical power transmission. First experiments have shown the relevance of this approach. In near future, clinical trials will be realized on this device.

References

1. Bottlang, M., Madey, S.M., Steyers, C.M., Marsh, J.L., Brown, T.D.: Assessment of elbow joint kinematics in passive motion by electromagnetic motion tracking. *J. Orthop. Res.* 612–618 (2011)
2. Cai, V.A.D., Bidaud, P., Hayward, V., Gosselin, F.: Method for the Identification of anatomical joint motion based on a six degree of freedom electro-goniometer. In:

- ROMANSY 18—Robot Design, Dynamics and Control, vol. 524, pp. 399–406, Udine-Italia (2010)
3. Cai, V.A.D., Bidaud, P., Hayward, V., Gosselin, F., Desailly, E.: Self-adjusting Isostatic exoskeleton for the human knee joint. In: Annual International Conference of the IEEE Engineering in Medicine and Biology Society, pp. 612–618 (2011)
 4. Chablat, D., Angeles, J.: The computation of all 4R serial spherical wrists with an isotropic architecture. *J. Mech. Des.* **25**(2), 275–280 (2003)
 5. Ergin, M.A., Patoglu, V.: A self-adjusting knee exoskeleton for robot-assisted treatment of knee injuries. In: IEEE/RSJ International Conference on Intelligent Robots and Systems (IROS), pp. 4917–4922 (2011)
 6. Ericson, A., Arndt, A., Stark, A., Wretenberg, P., Lundberg, A.: Variation in the position and orientation of the elbow flexion axis. *J. Bone Joint Surg.* **85-B**(4), 538–544 (2003)
 7. Jarrassé, N., Morel, G.: Formal methodology for avoiding hyperstaticity when connecting an exoskeleton to a human member. In: IEEE International Conference on Robotics and Automation (ICRA'10) (2010)
 8. Schiele, A., Van der Helm, F.C.T.: Kinematic design to improve ergonomics in human machine interaction. *IEEE Trans. Neural Syst. Rehabil. Eng.* **14**(4), 456–469 (2006)
 9. Stienen, A.H.A., Hekman, E.E.G., Van der Helm, F.C.T., Van der Kooij, H.: Self-aligning exoskeleton axes through decoupling of joint rotations and translations. *IEEE Trans. Robot.* **25**, 628–633 (2009)
 10. Woltring, H.J., Huiskes, R., De Lange, A.: Finite centrode and helical axis estimation from noisy landmark measurements in the study of human joint kinematics. *J. Biomech.* **18**(5), 379–389 (1985)

Design of Ankle Rehabilitation Mechanism Using a Quantitative Measure of Load Reduction

Daisuke Matsuura, Shouta Ishida, Tatsuya Koga
and Yukio Takeda

Abstract In order to achieve a desired flexion motion with adjustable load and to provide objective measure of recovery status which is important to verify the condition of therapeutic exercise to support physiotherapists, as well as to establish self-rehabilitation by patients themselves, a simple spatial rehabilitation mechanism based on an extended Oldham's coupling was employed. A kinetostatic analysis was performed to determine reasonable values of design parameters to achieve practical working range for therapeutic exercises without exerting unnecessarily large joint load. By utilizing the analysis scheme, adjustment of the joint load by attaching passive springs was also conducted, and a quantitative measure of load reduction ratio was formulated to evaluate the effectiveness of the additional springs. Reduction efficiency among several different configurations of link length was compared to search for the possibility to find an optimum design considering both compactness and safeness of the rehabilitation device.

Keywords Rehabilitation robotics · Ankle joint rehabilitation · Mechanism design · Kinetostatic analysis · Passive adaptation to spatial eccentricity of human joint

1 Introduction

In the coming highly-aged society, increasing of dependents on caregivers will become a big issue. To solve this problem, recovery and enhancement of body functions of elderly people is important, since they are likely to become bedridden due to the weakening of their lower limb. For prompt therapeutic exercises,

D. Matsuura (✉) · S. Ishida · T. Koga · Y. Takeda
Department of Mechanical Sciences and Engineering, Tokyo Institute of Technology,
2-12-1 Ookayama, Meguro-ku, Tokyo 152-8552, Japan
e-mail: matsuura@mech.titech.ac.jp

physiotherapists (PT) need effective treatment protocols based on objective measures of mobilization as well as on exerted and resistant force and torque on affected parts. With this information, PTs can decide on suitable exercise programs.

In order to carry out safe rehabilitation, inadequate conditions called *misuse* caused by unnecessary joint load should be suppressed. It is well known that human's joint has complicated structure, and its spatial movement is thus also complicated and has no constant axis of rotation [1, 2]. Many specially-designed mechanisms have been developed to adapt to the motion of joint axis, e.g. making offset to match the orthosisrotation center to user's joint [3], planar 6-DOF closed-loop mechanism [4], grooved cams and non-circular gears [5]. However, these apparatuses have to be custom-made to fit each user. This requirement can be satisfied by introducing self-adapting features e.g. a combination of two-prismatic joints [6] or a series of P-R-P joints [7], but such features entail more DOFs than the motion of target joints, and thus make the apparatuses complicated, heavy, and expensive. In addition, they cannot adapt to spatial motions.

To solve these problems, the authors have proposed an effective solution by introducing a simple spatial mechanism capable of passively adapting to an eccentricity of user's joint axis, and adjustment of exerted load by attaching passive spring [8]. As an important and practical application, dorsiflexion (DF) and plantar flexion (PF) of user's ankle joint was attempted, but design parameters have not been proofed by quantitative evaluations. In this paper, a reasonable link length to fit to user's physique while achieving practical ROM will be newly determined, and properties of additional springs to achieve effective reduction of the joint load will also be found through a kinetostatic analysis. An evaluation index of reduction ratio of the ankle joint load will be calculated regarding several different combinations of design parameter values to demonstrate the possibility to find out an optimum design regarding the compactness and safeness of the device.

2 Synthesis of the Rehabilitation Mechanism

There are four phases in typical therapeutic exercises of ankle joint which need to restore its range of motion (ROM) after tendon injury or high sprain [9]. Since the allowable range of motion and joint load in each phase are different, PTs manage ROM and joint load during the exercises based on their haptic sensations. The mechanism proposed in this paper aims to achieve suitable ROM and joint load at each phase just like PTs are doing. First, required ROM for the mechanism was determined by analyzing the movement of the human ankle joint using an optical 3D motion capture setup (MAC3D, Motion Analysis Corp.). From the result of the analysis and literature values shown in Table 1 [10–12], required angular amplitudes in plantar-dorsi and inversion–eversion axes for the mechanism have been determined to be $\pm 30^\circ$ and $\pm 10^\circ$, respectively.

Table 1 Range of motion of healthy ankle joint (unit: °)

Direction	Maximum	Functional
Plantar–Dorsi	$-20^\circ < \theta < 45^\circ$	$-10^\circ < \theta < 20^\circ$
Inversion–Eversion	$-25^\circ < \varphi < 35^\circ$	$-10^\circ < \varphi < 10^\circ$

As mentioned above, the mechanism must be capable of avoiding unnecessary joint load, namely shear, tensile and compressive force, while transmitting only torque from an input link to the ankle joint. To satisfy this requirement, Oldham's coupling mechanism can be effective. Figure 1 is a conceptual schematic drawing of the mechanism. Since the user's leg and foot are fixed on links, the user's body and the mechanism form a monolithic mechanical system. In the drawing, ankle joint is represented by a virtual joint J_7 , of which location changes continuously with respect to the orientation change of the foot, and there is also a virtual link between the joints J_6 and J_7 . The degrees of freedom (DOF) of the system can be calculated with Gruebler's equation,

$$F = F_s(N - 1) - \sum_{f=1}^{F_s-1} (F_s - f)P_f. \quad (1)$$

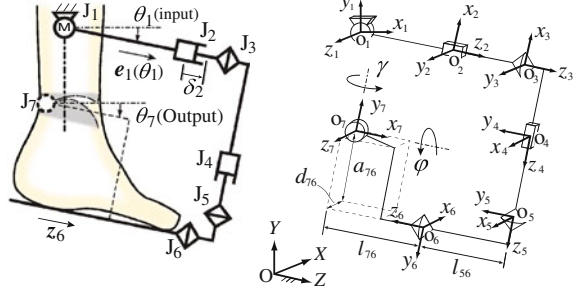
where F_s is the DOF of the workspace, N is the number of links, and P_f is the number of joints having f -DOF. By substituting $F_s = 6$, $N = 5$, and $P_1 = 3$ and $P_2 = 2$ to the equation, DOF of the mechanism becomes 1. In contrast, when the mechanism is detached from the user's leg, the virtual link and virtual joint J_7 are disappeared, and the value of N and P_1 become 4 and 2, respectively. As the result, DOF of the mechanism becomes 6, which is the same as DOF of the workspace. This means that the mechanism is settled only when the mechanism is attached to user's leg, and can drive the user's foot with any the location and direction of the rotation center of user's ankle joint, while passively adapting to fluctuation.

3 Kinetostatic Analysis of the Mechanism

3.1 Kinematic Analysis

A kinematic analysis is performed using several parameters and coordinate systems illustrated in Fig. 1 to obtain the relationship between the input angle, θ_1 , and output angle, θ_7 . Although all the coordinate axes are drawn as they are parallel with each other, they can take arbitrary directions due to the actual design and spatial motion of the mechanism. The rotation of the virtual joint J_7 around x_7 and y_7 axes are evaluated as φ and γ , respectively. First of all, location of all joints and the distance between J_1 and J_7 are denoted as $\mathbf{r}_{i=1\dots7} = [x_i \ y_i \ z_i]^T$ and $d = \sqrt{d_x^2 + d_y^2 + d_z^2}$, respectively. Since the location of J_7 in O-XYZ coordinate can be noted as $[x_7 \ y_7 \ z_7]^T = [x_1 + d_x \ y_1 + d_y \ z_1 + d_z]^T$, that of J_3 and J_5 are described as:

Fig. 1 The special rehabilitation mechanism and given coordinate system



$$r_3 = \delta_2 e_1 + r_1, \quad r_5 = (r_6 - r_7) + l_{56} z_6, \quad (2)$$

where δ_2 , l_{56} , e_1 and z_6 denote the displacement of joint J_2 , distance between J_5 and J_6 , a unit vector toward J_3 from J_1 , and a unit vector toward J_5 from J_6 . The coordinate rotation from $O_1 - x_1 y_1 z_1$ to $O_7 - x_7 y_7 z_7$ is written as:

$$R_x(\gamma)R_z(\varphi) = \begin{bmatrix} \cos \gamma & \sin \gamma \cos \varphi & \sin \gamma \sin \varphi \\ 0 & \cos \varphi & -\sin \varphi \\ -\sin \gamma & \cos \gamma \sin \varphi & \cos \gamma \cos \varphi \end{bmatrix}. \quad (3)$$

From the relationships between certain links, $J_2 J_3 \perp J_3 J_5$ and $J_4 J_5 \perp J_5 J_6$,

$$e_1 \cdot (r_3 - r_5) = 0, \quad z_6 \cdot (r_3 - r_5) = 0 \quad (4)$$

can be obtained. By introducing parametric representations

$$\sin \theta_7 = \frac{2k}{1+k^2}, \quad \cos \theta_7 = \frac{1-k^2}{1+k^2}. \quad (5)$$

Equation (4) is written as the following quadric polynomial;

$$k^4(A_5 - A_1) + 2k^3(A_2 - A_3) + 2k^2(2A_4 - A_5) + 2k(A_2 - A_3) + (A_1 + A_5) = 0, \quad (6)$$

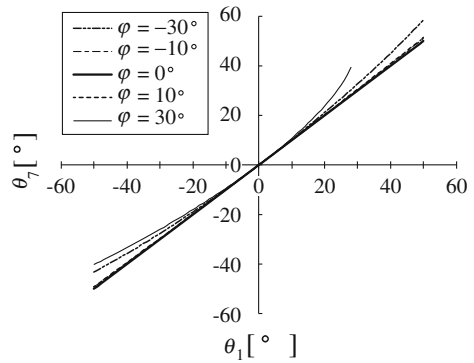
where $A_{1\dots 5}$ are constant terms determined by design parameters. For want of space, their detail is abbreviated except in case of A_1 ,

$$A_1 = d_x c(\theta_1) - d_z s(\gamma) - d_{67} s(\gamma) c(\gamma) c(\varphi) c^7(\theta_1) \\ + d_{67} c(\gamma) s(\varphi) s(\theta_1) c(\theta_1) - d_y c(\gamma) s(\theta_1) c(\theta_1) - d_x c(\gamma) c^2(\theta_1). \quad (7)$$

By solving Eqs. (5) and (6), input-output relationship of the mechanism is calculated in such a way that output angle, θ_7 , regarding given orientation angles of the ankle joint, γ and φ , and input angle, θ_1 , can be obtained. In order to fit the

Table 2 Design parameters
(unit: m)

Parameters	Value (m)
d_x	0.0
d_y	-0.1
d_z	0.15
l_{65}	0.053
l_{73}	0.1
a_{76}	0.1
d_{76}	-0.15

Fig. 2 Input–output relationship of the mechanism

mechanism to typical adult user's physique while minimizing its volume, essential design parameters are defined as Table 2. The input–output relationship in the range of $-30^\circ < \varphi < 30^\circ$ while holding $\gamma = 0$ is obtained as shown in Fig. 2. By comparing Fig. 2 and typical ROM of a healthy ankle joint shown in Table 1, it can be said that the rehabilitation mechanism will achieve linear input/output relationship within the functional region, $-10^\circ < \varphi < 10^\circ$.

3.2 Static Analysis

In order to estimate the load exerted on the ankle joint, static analysis was performed considering the gravitational force applied to each link and the friction of the two prismatic joints. According to the free-body diagram shown in Fig. 3, equilibrium of force and moment on the links are expressed as;

(a) Equilibrium of force:

$$\begin{aligned}
 F_1 - F_2 + m_1g - F_a &= 0, & F_2 - F_3 + m_2g + F_a - F_b &= 0, \\
 F_3 - F_4 + m_3g + F_b &= 0, & F_4 - F_5 + m_4g &= 0.
 \end{aligned}
 \tag{8}$$

Fig. 3 Free body diagram of the proposed mechanism

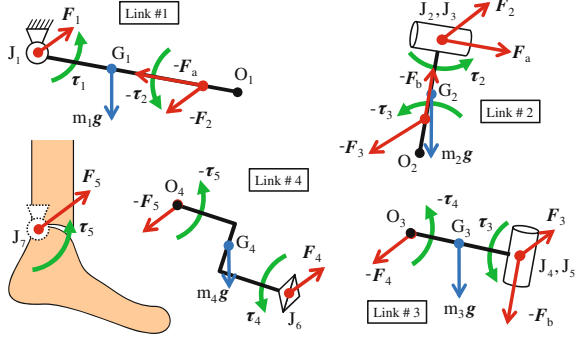


Table 3 Link mass

No.	Length (m)	Mass (kg)
1	0.30 (ℓ_{31})	0.089
2	0.25 (ℓ_{53})	0.074
3	0.05 (ℓ_{31})	0.044
4	$\left. \begin{array}{l} \mathbf{0.10}(\ell_{76}) \\ \mathbf{0.10}(\alpha_{76}) \\ \mathbf{0.15}(d_{76}) \end{array} \right\}$	0.425 + 3.075 [force sensor]

(b) Equilibrium of moment:

$$\begin{aligned} \tau_1 - \tau_2 + l_{g1} \times m_1 g - l_1 \times F_2 &= 0, & \tau_2 - \tau_3 + l_{g2} \times m_2 g - l_2 \times F_3 &= 0, \\ \tau_3 - \tau_4 + l_{g3} \times m_3 g - l_3 \times F_4 &= 0, & \tau_4 - \tau_5 + l_{g4} \times m_4 g - l_4 \times F_5 &= 0. \end{aligned} \quad (9)$$

where $m_{1\dots 4}$ and \mathbf{g} denote the mass of links #1,...,#4 and gravitational acceleration. \mathbf{l}_{g_i} and \mathbf{l}_i are the vectors pointing towards the i -th center of mass, G_i , and i -th end point, O_i , from J_1 , J_2 , J_4 and J_6 . From Eqs. (8) and (9), frictional force on the prismatic joints on J_2 and J_4 and the magnitude of ankle joint load are obtained:

$$F_a, F_b = \mu \sqrt{F_{\alpha,i}^2 + F_{\beta,i}^2} \Big|_{i=2,4}, \quad (10)$$

$$F_{load} = \sqrt{F_{7x}^2 + F_{7y}^2 + F_{7z}^2}, \quad (11)$$

where μ is a friction coefficient which is given as $\mu = 0.2$ in the following analysis. $\mathbf{F}_{\alpha,i}$ and $\mathbf{F}_{\beta,i}$ are the coaxial forces with respect to each link and its orthogonal force, respectively. In order to carry out the calculation, the mass of each link shown in Table 3 were substituted. Values in the table were calculated based on the assumption that all the links were made of carbon steel. Figure 4 plots

Fig. 4 Load on the ankle joint J_7

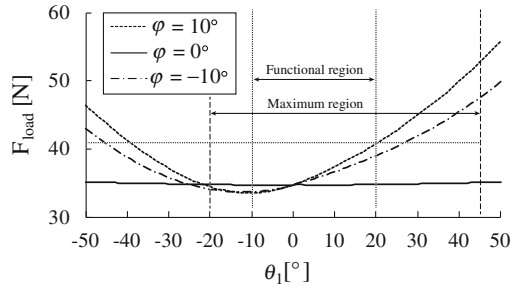
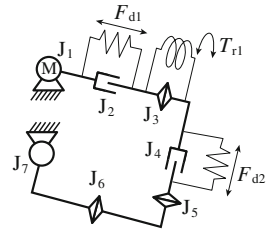


Fig. 5 Additional springs on J_2, J_3 and J_4



the relationship between the input angle θ_1 and the amplitude of F_{load} with respect to different inversion/eversion angles. The result indicates that the amplitude of the ankle joint load within the functional range was approximately 40 N at most.

4 Adjustment of Ankle Joint Load Using Passive Springs

Although it is difficult to completely avoid ankle load, it can be compensated by adding springs to certain joints. To select the joints to attach the springs, optimum amplitude and direction of compensation force on each joint to minimize F_{load} with respect to different θ_1 were firstly calculated. From the result of this calculation, it was found that springs on J_2, J_3 and J_4 are effective to reduce F_{load} . Since J_2 and J_4 are prismatic joints and J_3 is a revolute joint, suitable types of springs are attached as shown in Fig. 5. Next, spring coefficient and initial displacement of the three springs were determined by simply applying line-fitting to the distribution of the optimum compensation force/torque against displacement of each joint as shown in Fig. 6. The spring constant and initial length of each spring were therefore determined as shown in Table 4. The negative sign in the table indicates the direction of the spring force. In order to search for the possibility to optimize the length of each link, ankle load was calculated with several different combinations of d_y and l_{76} , 0.05 m longer and shorter ones than the original value in Table 2. The obtained ankle load in case of three different d_y is plotted in Fig. 7.

Fig. 6 Displacement/force relationship on J_2 at different foot orientations

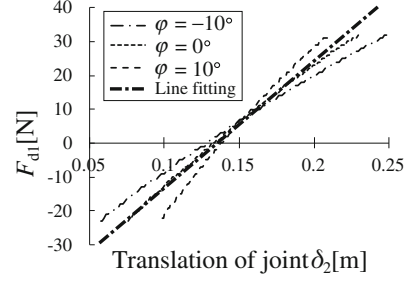
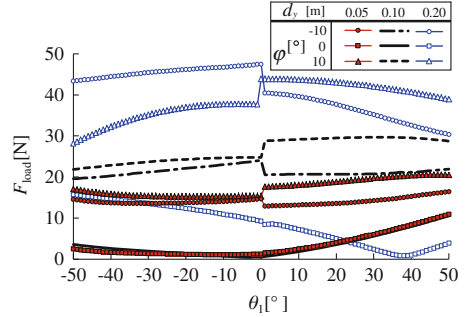


Table 4 Properties of the springs

No.	Type	Initial displacement	Spring coefficient
J_2	Tensile	-0.13 m	375.5 N/m
J_3	Torsional	0.09 rad	39.04 Nm/rad
J_4	Tensile	-0.14 m	393.0 N/m

Fig. 7 Compensated ankle load distribution with respect to different link length



The effectiveness of each configuration on the load reduction was evaluated by an index,

$$\eta = 1 - \frac{\sum_{j=1}^N (F_{load,j} - \hat{F}_{load,j})}{N \cdot F_{load}}, \quad (12)$$

where F_{load} and \hat{F}_{load} are the ankle load with and without the springs at the j -th sampling and N is the number of acquired data. Based on the value of η shown in Table 5, the ankle load was reduced 91 % at most or 34 % at least by attaching the springs, and the reduction ratio can be increased by using larger d_y . In case of $\underline{d}_y = 0.20$, F_{load} was less than 20 N among entire maximum ROM. That condition is suitable for typical therapeutic exercise shown in [9]. However, there is a trade-off

Table 5 Load reduction index η (%)

Ankle inclination φ (deg)		-10	0	10
Orig (d_y, ℓ_{76}) = (0.10, 0.10)		44	91	34
d_y (m)	Short (0.05)	-8	76	3
	Long (0.20)	63	90	57
ℓ_{76} (m)	Short (0.05)	24	89	7
	Long (0.20)	58	89	48

that increasing of link length will also enlarges the size of the rehabilitation apparatus. Optimum link length should be determined by considering both compactness and safeness. This adjustment technique can be used not only to reduce the load but also to exert a desired force. Furthermore, the resistance of a joint can be estimated by substituting the measured motion to the theoretical model. The estimated resistance will become useful information in evaluating the recovery status of joints and determining suitable rehabilitation programs for each patient.

5 Conclusion

This paper has discussed the design and analysis of a simple rehabilitation mechanism capable of adapting to fluctuation in the rotation axis and the adjusting of exerted load. The obtained results can be summarized as follows;

- (1) Based on the extended Oldham's coupling mechanism, a simple spatial rehabilitation mechanism which can transmit only driving torque while adapting to changes in the axis of rotation has been proposed. The composition of the 1-DOF mechanism is very simple and thus contributes to the development of a lightweight and inexpensive rehabilitation device.
- (2) A practical design of a prototype to achieve a desired working range was determined according to the result of human motion analysis experiments and literature data. Subsequently, a kinetostatic analysis considering the effects of gravitational force and friction on cylindrical joints was done to estimate the magnitude of the load on the joints.
- (3) Adjustment of ankle joint load by means of springs was introduced and a practical number, location and physical properties of springs were systematically determined. The result of our theoretical analysis with the spring configuration obtained was that the load force could be reduced greater than 34 %.
- (4) Possibility to determine optimum length to reduce joint load was shown by evaluating several different combination of design parameters. There is a trend that larger link length tends to achieve less joint load. However, since not only the compactness but also safeness should be paid attention to figure out practical design, those two factors should be simultaneously considered.

References

1. Malosio, M., et al.: Analysis of elbow-joints misalignment in upper-limb exoskeleton. In: IEEE International Conference on Rehabilitation Robotics, 2011
2. Gregorio, R., et al.: Mathematical models of passive motion at the human ankle joint by equivalent spatial parallel mechanisms. *Med. Biol. Eng. Compu.* **45**(3), 305–313 (2007)
3. Esmaili, M., et al.: Ergonomic considerations for anthropomorphic wrist exoskeletons: a simulation study on the effects of joint misalignment. In: Proceedings of the IEEE International Conference on Intelligent Robots and Systems, pp. 4905–4910 (2011)
4. Jin, D., et al.: Kinematic and dynamic performance of prosthetic knee joint using six-bar mechanism. *J. Rehab. Res. Dev.* **40**(1), 39–48 (2003)
5. Teradaet, H., et al.: Developments of a Knee Motion Assist Mechanism for Wearable Robot with a Non-circular Gear and Grooved Cams. *Mech. Mach. Sci.* **3**(2):69–76 (2012)
6. Stienen, A.H.A., et al.: Self-aligning exoskeleton axes through decoupling of joint rotations and translations. *IEEE Trans. Robot.* **25**(3):628–633 (2009)
7. Cai, D., et al.: Design of self-adjusting orthoses for rehabilitation. In: Proceedings of the IASTED International Conference on Robotics and Applications, pp. 215–223 (2009)
8. Matsuura, D., et al.: Kinetostatic design of ankle rehabilitation mechanism capable of adapting to changes in joint axis. *J. Robot. Mechatron.* **25**(6), 1029–1037 (2013)
9. Mattacola, C.G., et al.: Rehabilitation of the ankle after acute sprain or chronic instability. *J. Athl. Train.* **37**(4), 413–429 (2002)
10. Gao, F., Ren, Y., et al.: Effects of repeated ankle stretching on calf muscle-tendon and ankle biomechanical properties in stroke survivors. *Clin. Biomech.* **26**(5), 516–522 (2011)
11. Sekiguchi, Y., et al.: The contribution of quasi-joint stiffness of the ankle joint to gait in patients with hemiparesis. *Clin. Biomech.* **27**(5), 495–499 (2012)
12. Lee, H., Ho, P., et al.: Multivariable static ankle mechanical impedance with relaxed muscles. *J. Biomech.* **44**, 1901–1908 (2011)

Characterization of the Subsystems in the Special Three-Systems of Screws

Dimitar Zlatanov and Marco Carricato

Abstract The paper examines the subspaces of a space spanned by three independent twists (or wrenches) with axes parallel to a common plane. A complete characterization of all screw cylindroids nested within a special three-system of screws is given. The results are illustrated by means of geometric models of three-dimensional projective space incorporating the Ball circle diagram of the cylindroid.

Keywords Screw systems · Projective space · Mechanism synthesis

1 Introduction

In robotic systems, the possible instantaneous motions of a rigid body, or the systems of forces acting on it, are described by a subspace of the six-dimensional vector space of twists, or wrenches. Such linear subspaces, or the underlying projective spaces, are referred to as screw systems. Screw systems were first studied in [1], but a comprehensive classification and detailed geometrical characterizations were obtained in [6]. See also [4, 5, 7, 8].

Two screw systems are *equivalent* if one can be seen as a rigid-body displacement of the other. This relation divides the space of linear subspaces of $se(3)$ into infinitely many equivalence *classes*. Geometrically similar classes are grouped into *types*: one general and a variety of special, according to [6].

D. Zlatanov (✉)

DIME, University of Genoa, Genova, Italy

e-mail: zlatanov@dimec.unige.it

M. Carricato

DIN and ICIR-HST, University of Bologna, Bologna, Italy

e-mail: marco.carricato@unibo.it

Following Gibson and Hunt [5] a screw-system class can be labeled by: its dimension; I or II, indicating whether or not there are screws of more than one finite pitch; a letter (from A to D) denoting the number (from 0 to 3) of independent infinite-pitch screws; and additional parameters. In this paper we study three-systems of B- and C-types, such as the seventh special [6], i.e., class 3-IB(h_o, γ) with special pitch h_o and angle γ .

One aspect of screw-system geometry, not yet explored in detail, is the nesting of lower-rank systems within ones of higher dimension. The key issue is the characterization of all two-systems within a three-system. (Nesting in higher-rank systems reduces to lower dimensions via reciprocity.) For each three-system, one can ask: what two-subsystem classes have representatives, and where are these two-systems located? Such questions are of theoretical value and have practical relevance in mechanism analysis and synthesis: subspaces describe end-effector freedoms under additional constraints; the orbits of $SE(3)$ action in the Grassmanian are important when trying to find serial chains with a persistent screw-system class [3].

This paper examines the subspaces of any three-system whose screw axes are parallel to a plane. For those of A types, see [2]. In the most complex cases, 3-IB(h_o, γ) and 3-IB $^\circ$ (h_o), this is done via a novel way of representing the screws of the system as points on a plane.

2 Screws and Projective Spaces

A twist (or a wrench) is given by a pair of vectors, $(\boldsymbol{\omega}, \mathbf{v}) \in se(3)$, the body's angular velocity and the linear velocity at the origin (or $(\mathbf{f}, \mathbf{m}) \in se(3)^*$, the resultant force and moment at the origin). An element, $\boldsymbol{\xi} = (\boldsymbol{\omega}, \mathbf{v})$, of $se(3)$ (similarly $se(3)^*$) is associated with a *screw* about which the body twists (or the wrench is applied)—a line in space, $\ell(\boldsymbol{\xi})$, the screw axis, with a metric scalar, the pitch h , given by

$$h = \frac{\boldsymbol{\omega} \cdot \mathbf{v}}{\boldsymbol{\omega} \cdot \boldsymbol{\omega}}, \quad \mathbf{r}_\perp = \frac{\boldsymbol{\omega} \times \mathbf{v}}{\boldsymbol{\omega} \cdot \boldsymbol{\omega}} \quad (1)$$

where \mathbf{r}_\perp is the axis point closest to the origin. Conversely, $\boldsymbol{\xi} = (\boldsymbol{\omega}, \mathbf{v}) = (\boldsymbol{\omega}, h\boldsymbol{\omega} + \mathbf{r} \times \boldsymbol{\omega})$, for any $\mathbf{r} \in \ell(\boldsymbol{\xi})$. An infinite-pitch screw is a pure direction of a translation $(0, \mathbf{v})$ (or a force couple $(0, \mathbf{m})$).

Each screw is identified with a class, $[\boldsymbol{\xi}]$, of twists obtained from each other by (real-number) scalar multiplication, i.e., it is an element of the five-dimensional *real projective space*, $[\boldsymbol{\xi}] \in P(se(3))$, generated by $se(3)$. Real projective n -space, $P(\mathbb{R}^{n+1}) = \mathbb{RP}^n$, is defined by imposing the equivalence relation $\mathbf{x} \sim \lambda\mathbf{x}$, $\lambda \neq 0$, on $\mathbb{R}^{n+1} - \{0\}$, identifying vectors that are scalar multiples. The equivalence classes can be thought of as lines through the origin in \mathbb{R}^{n+1} .

It is often desirable to visualize the elements of projective n -space as points of an n -manifold. One classic way is the so-called straight model, which maps $\mathbb{R}\mathbb{P}^n$ onto \mathbb{R}^n with an added hyperplane at infinity, by intersecting the lines (in \mathbb{R}^{n+1}) through the origin with an n -plane away from it. The *prestereographic model* [9] uses a sphere $S^n(s)$, with antipodal points O and some $s \in \mathbb{R}^{n+1}$. For a line through O not tangent to $S^n(s)$, we take the second intersection point as the image. The lines tangent to the sphere at the origin have no such second point, and so the image space needs to be augmented by “blowing-up” the origin and replacing it with a copy of $\mathbb{R}\mathbb{P}^{n-1}$. The sphere $S^n(s)$ can then be mapped onto a hyperplane via stereographic projection from the antipode, s . If $n = 2$ this results in a plane image (a circle inversion of the straight model) with a single point at infinity and a finite point blown-up. In Sects. 4 and 5 we use two models which map a three-system onto exactly such an image: a single-point-compactified plane with one other point blown-up.

3 The Ball Circle of the General Two-System

The screw system, $\mathcal{P}^1 = P(\mathcal{A}^2)$, of a two-dimensional subspace $\mathcal{A}^2 \subset se(3)$, is classified as *general*, when it has a pair of generators, $\mathcal{A}^2 = \text{Span}(\xi_1, \xi_2)$, on the *principal screws* of the system, with different finite pitches, $h_1 > h_2$, and intersecting perpendicular axes. In a coordinate frame with Ox and Oy along these axes:

$$\xi_1 = (\mathbf{i}, h_1\mathbf{i}), \quad \xi_2 = (\mathbf{j}, h_2\mathbf{j}) \quad (2)$$

$$\xi = c_\theta \xi_1 + s_\theta \xi_2 = (c_\theta \mathbf{i} + s_\theta \mathbf{j}, h_1 c_\theta \mathbf{i} + h_2 s_\theta \mathbf{j}) \quad (3)$$

with $c_\theta = \cos \theta$, $s_\theta = \sin \theta$, where θ is the screw-axis direction angle from Ox .

It is easy to obtain the pitch and the axis location:

$$h = h_2 + Hc_\theta^2, \quad \mathbf{r}_\perp = Hc_\theta s_\theta \mathbf{k} \quad (4)$$

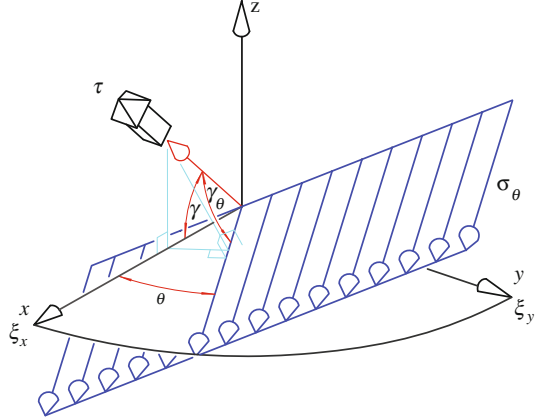
where $H = h_2 - h_1$. Eliminating θ we obtain

$$\left(p - \frac{H}{2}\right)^2 + z^2 = \frac{H^2}{4} \quad (5)$$

the equation of a circle in the (z, p) plane. This *Ball circle*, models geometrically the relationship between screw-axis location and pitch in the cylindroid [1, 6, 9]. It can be shown to be a prestereographic model of \mathcal{P}^1 [9]. This reflects the fact that the angle between the (projected) axes of any two screws is subtended by the arc between their image points on the circle.

Since translations in the (z, p) plane will just shift a circle, it follows that the two-system can be represented with a circle of the same size in a plane (Z, h) ,

Fig. 1 The axes of the screws with any given direction, θ , in 3-IB (h_o, γ) form a plane, σ_θ .



where h is the absolute pitch (rather than the relative, p) and Z is the elevation with respect to some arbitrary horizontal zero plane (rather than the central plane of the cylindroid identified with Oxy in the special coordinate system chosen above). This allows various different two-systems, with screws normal to a common direction, to be represented as circles on the same pitch-to-elevation plane.

In fact, some three-systems can be faithfully parameterized by the pair (z, p) [10]. In all such models, general two-systems appear as circles in the parameter plane. Moreover, this will be true after any change of variables which maps circles into circles, e.g., reflections, rotations, and dilations can be used. One novel such parameterization yielding a useful planar model is introduced in the following section.

4 Model and Subsystems of the Seventh-Special Three-System

A seventh-special three-system, class 3-IB (h_o, γ) [5, 6], has basis and generic twist

$$\xi_x = (\mathbf{i}, h_o \mathbf{i}), \quad \xi_y = (\mathbf{j}, h_o \mathbf{j}), \quad \tau = (0, c_\gamma \mathbf{i} + s_\gamma \mathbf{k}) \quad (6)$$

$$\xi = c_\theta \xi_x + s_\theta \xi_y + m\tau = (c_\theta \mathbf{i} + s_\theta \mathbf{j}, (h_o c_\theta + m c_\gamma) \mathbf{i} + h_o s_\theta \mathbf{j} + m s_\gamma \mathbf{k}) \quad (7)$$

The system's finite-pitch screws are all parallel to Oxy , Fig. 1. Those with pitch h_o form two pencils: concurrent at O in Oxy and a Oy -parallel in the plane through Oy normal to $c_\gamma \mathbf{i} + s_\gamma \mathbf{k}$.

For the pitch and the axis location of ξ we have:

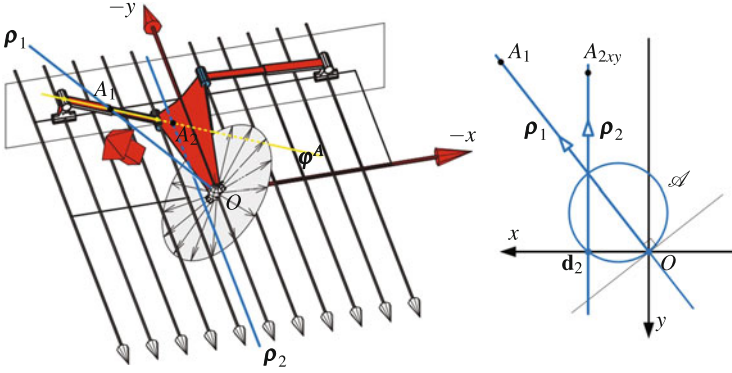


Fig. 2 The freedoms, $\mathcal{S} = \text{Span}(\rho_1, \rho_2)$, of the Exechon platform with a blocked actuator

$$h = h_o + p = h_o + mc_\theta c_\gamma \quad (8)$$

$$\mathbf{r}_\perp = \mathbf{d} + z\mathbf{k} = m(s_\theta s_\gamma \mathbf{i} - c_\theta s_\gamma \mathbf{j}) - ms_\theta c_\gamma \mathbf{k}. \quad (9)$$

We notice that almost every finite-pitch screw is defined univocally by the projection, \mathbf{d} , of \mathbf{r}_\perp on Oxy . The only exceptions are the screws in the central h_o -pitch pencil at O , for which $\mathbf{d} = 0$. Thus we can use the plane (d_x, d_y) with point O blown up (to include the concurrent h_o -pencil) and an added single point at infinity (to represent the ∞ -screw) as a model of the three-system. Moreover, since

$$\mathbf{d} = d_x \mathbf{i} + d_y \mathbf{j} = -z(\tan \gamma) \mathbf{i} - p(\tan \gamma) \mathbf{j} \quad (10)$$

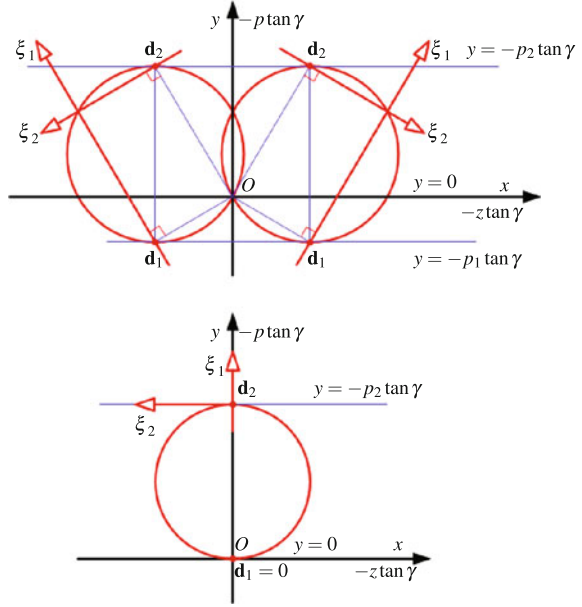
this geometric representation also describes the pitch and location of the screw.

From what was said in the previous section, general two-subsystems are mapped into circles in the (d_x, d_y) plane. Each such circle must pass through O , because every two-subsystem includes a screw in the central pencil. (Every two projective two-subspaces in a three-space intersect.)

For example, the platform twists of the Exechon tripod form a 3-IB(0, γ) system in almost every configuration, (including the singular one in) Fig. 2 [11]. If an actuator is blocked, the constraint-wrench basis can be augmented by the pure force along the leg, φ^A , shown in Fig. 2—left with the original concurrent and planar force pencils. This leaves only a two-system of freedoms, \mathcal{S} , spanned by rotations ρ_1 and ρ_2 , with axes intersected by $\ell(\varphi)^A$. In the model plane, Fig. 2—right, \mathcal{S} is the circle through the image point \mathbf{d}_2 of ρ_2 , and with tangent at O perpendicular to the direction of ρ_1 direction at O .

The principal screws of a general two-subsystem are represented on the circle by the antipodal points with tangents parallel to Ox . Conversely, given $h_1 > h_2$, a nested 2-IA (h_1, h_2) system is given by a circle tangent to the $(Ox$ -parallel) lines $d_y = y = -(h_i - h_o) \tan \gamma$, $i = 1, 2$. If $h_o > h_1$ or $h_2 > h_o$, there is *no solution*,

Fig. 3 Nested general two-subsystem in 3-IB(h_o, γ): top $h_1 > h_o > h_2$; bottom $h_1 = h_o$



when $h_o = h_i$ there is a *unique solution*, and when $h_1 > h_o > h_2$ there are *exactly two subsystems* of this class, Fig. 3. The elevation, z , and the Oxy projection, \mathbf{r} , of the center are

$$z = \varepsilon \sqrt{(h_1 - h_o)(h_o - h_2)} \quad (11)$$

$$\mathbf{r} = \varepsilon \tan \gamma (2\sqrt{(h_1 - h_o)(h_o - h_2)} \mathbf{i} + (h_1 - h_2) \mathbf{k}), \quad \varepsilon = \pm 1. \quad (12)$$

The special two-subsystems are: the 2-II(h_o) central pencil in Oxy ; the IIB (h_o) parallel pencil in a plane through Oy normal to $c_\gamma \mathbf{i} + s_\gamma \mathbf{k}$ (the abscissa axis in the model); and two representatives of each class 2-IB(β) with $\gamma < \gamma_\theta = \beta < \pi/2$, Fig. 1.

5 Model and Subsystems of the Eighth-Special Three-System

A system of class 3-IB $^\circ$ (h_o) (eighth-special in [6]) is spanned by $\xi_x = (\mathbf{i}, h_o \mathbf{i})$, $\xi_y = (\mathbf{j}, h_o \mathbf{j})$, and $\tau_z = (0, \mathbf{i})$, Fig. 4. For finite-pitch normalized twists in the system,

$$\xi = c_\theta \xi_x + s_\theta \xi_y + m \tau_z = (c_\theta \mathbf{i} + s_\theta \mathbf{j}, (h_o c_\theta + m) \mathbf{i} + h_o s_\theta \mathbf{j}) \quad (13)$$